INFLUENCE OF HETEROTROPHIC BACTERIA AND OTHER SUB-MICROMETER PARTICLES ON LIGHT SCATTERING IN THE OCEAN

by

Osvaldo Ulloa

Submitted in partial fulfillment of the requirements
for the degree of Doctor of Philosophy

at

Dalhousie University
Halifax, Nova Scotia
November, 1992

ISBN 0-315-80153-0

Name OSVALDO ULLOA

Dissertation Abstracts International is arranged by broad, general subject categories. Please select the one subject which most nearly describes the content of your dissertation. Enter the corresponding four digit code in the spaces provided.

OCEANOGRAPHY — 0416 & 0415

SUBJECT TERM — SUBJECT CODE

UMI

Subject Categories

THE HUMANITIES AND SOCIAL SCIENCES

COMMUNICATIONS AND THE ARTS

Architecture	0729
Art History	0377
Cinema	0900
Dance	0378
Fine Arts	0357
Information Science	0723
Journalism	0391
Library Science	0399
Mass Communications	0708
Music	0413
Speech Communication	0459
Theater	0465

EDUCATION

General	0515
Administration	0514
Adult and Continuing	0516
Agricultural	0517
Art	0273
Bilingual and Multicultural	0282
Business	0688
Community College	0275
Curriculum and Instruction	0727
Early Childhood	0518
Elementary	0524
Finance	0277
Guidance and Counseling	0519
Health	0680
Higher	0745
History of	0520
Home Economics	0278
Industrial	0521
Language and Literature	0279
Mathematics	0280
Music	0522
Philosophy of	0998
Physical	0523
Psychology	0525
Reading	0535
Religious	0527
Sciences	0714
Secondary	0533
Social Sciences	0534
Sociology of	0340
Special	0529
Teacher Training	0530
Technology	0710
Tests and Measurements	0288
Vocational	0747

LANGUAGE, LITERATURE AND LINGUISTICS

Language	
General	0679
Ancient	0289
Linguistics	0290
Modern	0291
Literature	
General	0401
Classical	0294
Comparative	0295
Medieval	0297
Modern	0298
African	0316
American	0591
Asian	0305
Canadian (English)	0352
Canadian (French)	0355
English	0593
Germanic	0311
Latin American	0312
Middle Eastern	0315
Romance	0313
Slavic and East European	0314

PHILOSOPHY, RELIGION AND THEOLOGY

Philosophy	0422
Religion	
General	0318
Biblical Studies	0321
Clergy	0319
History of	0320
Philosophy of	0322
Theology	0469

SOCIAL SCIENCES

American Studies	0323
Anthropology	
Archaeology	0324
Cultural	0326
Physical	0327
Business Administration	
General	0310
Accounting	0272
Banking	0770
Management	0454
Marketing	0338
Canadian Studies	0385
Economics	
General	0501
Agricultural	0503
Commerce Business	0505
Finance	0508
History	0509
Labor	0510
Theory	0511
Folklore	0358
Geography	0366
Gerontology	0351
History	
General	0578
Ancient	0579
Medieval	0581
Modern	0582
Black	0328
African	0331
Asia Australia and Oceania	0332
Canadian	0334
European	0335
Latin American	0336
Middle Eastern	0333
United States	0337
History of Science	0585
Law	0398
Political Science	
General	0615
International Law and Relations	0616
Public Administration	0617
Recreation	0814
Social Work	0452
Sociology	
General	0626
Criminology and Penology	0627
Demography	0938
Ethnic and Racial Studies	0631
Individual and Family Studies	0628
Industrial and Labor Relations	0629
Public and Social Welfare	0630
Social Structure and Development	0700
Theory and Methods	0344
Transportation	0709
Urban and Regional Planning	0999
Women s Studies	0453

THE SCIENCES AND ENGINEERING

BIOLOGICAL SCIENCES

Agriculture	
General	0473
Agronomy	0285
Animal Culture and Nutrition	0475
Animal Pathology	0476
Food Science and Technology	0359
Forestry and Wildlife	0478
Plant Culture	0479
Plant Pathology	0480
Plant Physiology	0817
Range Management	0777
Wood Technology	0746
Biology	
General	0306
Anatomy	0287
Biostatistics	0308
Botany	0309
Cell	0379
Ecology	0329
Entomology	0353
Genetics	0369
Limnology	0793
Microbiology	0410
Molecular	0307
Neuroscience	0317
Oceanography	0416
Physiology	0433
Radiation	0821
Veterinary Science	0778
Zoology	0472
Biophysics	
General	0786
Medical	0760

EARTH SCIENCES

Biogeochemistry	0425
Geochemistry	0996
Geodesy	0370
Geology	0372
Geophysics	0373
Hydrology	0388
Mineralogy	0411
Paleobotany	0345
Paleoecology	0426
Paleontology	0418
Paleozoology	0985
Palynology	0427
Physical Geography	0368
Physical Oceanography	0415

HEALTH AND ENVIRONMENTAL SCIENCES

Environmental Sciences	0768
Health Sciences	
General	0566
Audiology	0300
Chemotherapy	0992
Dentistry	0567
Education	0350
Hospital Management	0769
Human Development	0758
Immunology	0982
Medicine and Surgery	0564
Mental Health	0347
Nursing	0569
Nutrition	0570
Obstetrics and Gynecology	0380
Occupational Health and Therapy	0354
Ophthalmology	0381
Pathology	0571
Pharmacology	0419
Pharmacy	0572
Physical Therapy	0382
Public Health	0573
Radiology	0574
Recreation	0575
Speech Pathology	0460
Toxicology	0383
Home Economics	0386

PHYSICAL SCIENCES

Pure Sciences

Chemistry	
General	0485
Agricultural	0749
Analytical	0486
Biochemistry	0487
Inorganic	0488
Nuclear	0738
Organic	0490
Pharmaceutical	0491
Physical	0494
Polymer	0495
Radiation	0754
Mathematics	0405
Physics	
General	0605
Acoustics	0986
Astronomy and Astrophysics	0606
Atmospheric Science	0608
Atomic	0748
Electronics and Electricity	0607
Elementary Particles and High Energy	0798
Fluid and Plasma	0759
Molecular	0609
Nuclear	0610
Optics	0752
Radiation	0756
Solid State	0611
Statistics	0463

Applied Sciences

Applied Mechanics	0346
Computer Science	0984
Engineering	
General	0537
Aerospace	0538
Agricultural	0539
Automotive	0540
Biomedical	0541
Chemical	0542
Civil	0543
Electronics and Electrical	0544
Heat and Thermodynamics	0348
Hydraulic	0545
Industrial	0546
Marine	0547
Materials Science	0794
Mechanical	0548
Metallurgy	0743
Mining	0551
Nuclear	0552
Packaging	0549
Petroleum	0765
Sanitary and Municipal	0554
System Science	0790
Geotechnology	0428
Operations Research	0796
Plastics Technology	0795
Textile Technology	0994

PSYCHOLOGY

General	0621
Behavioral	0384
Clinical	0622
Developmental	0620
Experimental	0623
Industrial	0624
Personality	0625
Physiological	0989
Psychobiology	0349
Psychometrics	0632
Social	0451

A Sophie y mis padres

TABLE OF CONTENTS

LIST OF FIGURES

LIST OF TABLES

ABSTRACT

Mie theory is applied to estimate scattering by polydispersions of marine particles, with particular emphasis on heterotrophic bacteria and sub-micrometer detrital particles.

The error incurred in deriving bacterial optical properties by use of the simpler approximations of van de Hulst is computed. Simple approximations are derived for the scattering coefficient due to bacteria with normal and gamma size distributions. The scattering properties of natural bacterial assemblages in three marine environments, Georges Bank, Northeast Channel, and Sargasso Sea, are assessed by applying Mie theory to field data on bacterial size and abundance. Results show that heterotrophic bacteria can contribute significantly to both the total scattering coefficient and the backscattering coefficient of sea water, but that their contribution to the backscattering coefficient is relatively lower. The relative contribution of bacteria to the scattering properties of sea water was found to be unrelated to the amount of phytoplankton pigments present in the water.

The backscattering ratio (ratio between the backscattering coefficient and the total scattering coefficient) for the total particle suspension with a Junge-type size distribution was found to be largely controlled by sub-micrometer particles, and its magnitude to vary strongly with the value of the exponent in the Junge-type distribution, which in turn describes the shape of the size distribution. The backscattering ratio, however, does not vary with wavelength, nor is it significantly affected by absorption. It is predicted that even if sub-micrometer detrital particles, and not phytoplankton, are responsible for most of the backscattering in the ocean, an inverse relationship between the backscattering ratio and phytoplankton pigment concentration would exist, due to the observed inverse relationship between phytoplankton pigments and the parameter that describes the shape of the size distribution.

LIST OF SYMBOLS

a	Total absorption coefficient
a'	Absorption coefficient of the particle material
a_h	Absorption coefficient due to heterotrophic bacteria
a_w	Absorption coefficient due to water
a_k, b_k	Mie complex coefficients
b	Total scattering coefficient
b'	Particle scattering coefficient
b_h	Scattering coefficient due to heterotrophic bacteria
b_w	Scattering coefficient due to water
b_b	Total backscattering coefficient
b'_b	Particle backscattering coefficient
$\tilde{b}_b$	Total backscattering ratio
$\tilde{b}'_b$	Particle backscattering ratio
b_{bh}	Backscattering coefficient due to heterotrophic bacteria
b_{bw}	Backscattering coefficient due to water
c	Total (beam) attenuation coefficient
C	Phytoplankton pigment concentration
D	Equivalent spherical diameter
D_k	Logarithmic derivative
$f(D)$, $f(x)$	Probability density function
$F(D)$	Size distribution function
i^n	Complementary error function integral
$i_1(\theta)$, $i_2(\theta)$	Mie (dimensionless) angular intensity functions
j_k, y_k	Spherical bessel functions of the first and second kind
J_ν	Bessel function (of the first kind) of order ν
K	Coefficient in the Junge-type distribution
m	Complex refractive index with respect to the surrounding medium

m_w	Complex refractive index of water
n	Real part of the refractive index
n_w	Real part of the refractive index of water
n'	Imaginary part of the refractive index
N	Number concentration per unit volume
P_k	Legendre polynomial of order k
Q_a	Efficiency factor for absorption
Q_b	Efficiency factor for scattering
Q_{b_b}	Efficiency factor for backscattering
Q_c	Efficiency factor for attenuation
$\bar{Q}_j$	Effective efficiency factor for $j = a, b, c$, or b_b
r	Thickness of layer in the definition of inherent optical properties
s	Geometrical cross section
$S_1(\theta)$, $S_2(\theta)$	Mie (dimensionless) complex amplitude functions
U_ϑ	Parabolic cylinder function of order ϑ
x	(Dimensionless) size parameter
$\bar{x}$	Mean size parameter for a polydispersion
α_j	(Dimensionless) coefficients for approximation of $Q_b(x)$
$\beta(\vartheta)$	Total volume scattering function
$\beta_h(\theta)$	Volume scattering function due to heterotrophic bacteria
η, ν	Parameters of the gamma distribution
θ	Scattering angle
λ	Wavelength of light in vacuum
μ	Cosine of the scattering angle θ
$(\nu)_k$	Pochhammer polynomial of order k and argument ν
ξ	Coefficient in the Junge-type distribution
ρ, ρ'	van de Hulst's normalized size parameters
σ_x	Standard deviation of x for a polydispersion
$\tau_k(\mu)$, $\pi_k(\mu)$	Mie angular functions

ϕ_o	Incident ratiant flux
$d\phi_a$	Radiant flux absorbed
$d\phi_b$	Radiant flux scattered
$d\phi(\theta)$	Radiant flux scattered into an element of solid angle oriented at an angle θ
ψ_k, ζ_k, χ_k	Riccatti-Bessel functions of order k
$d\omega$	Element of solid angle

ACKNOWLEDGEMENTS

I would like to thank Dr. Trevor Platt and Dr. Shubha Sathyendranath for their continuous advice and guidance during the course of this thesis. I would also like to thank Dr. Dan Kelley and Dr. Marlon Lewis, the other two members of my supervisory committee, for their helpful comments.

I am grateful to all the scientific and technical staff at the Biological Oceanographic Division of the Bedford Institute of Oceanography. In particular, I would like to thank Dr. George White for his help with the computational aspects of this work. Thanks also to Renato Quiñones for providing me with the data on bacterial size and abundance.

Financial support during the course of this work was provided by the International Development Research Centre (IDRC), the Department of Fisheries and Oceans, and the Natural Sciences and Engineering Research Council through operating grants to Dr. Shubha Sathyendranath and Dr. Trevor Platt.

The friendship and support of many people made these years as a graduate student particularly enjoyable; muchas gracias! to all of them. Most of all I want to thank Sophie and my parents for their love, support, patience, and understanding.

General Introduction

Knowledge of the optical (absorption and scattering) properties of the different substances present in sea water (both in solution and in suspension) is necessary to address problems such as: the interpretation and modelling of ocean colour for remote sensing of phytoplankton (Morel and Prieur, 1977; Gordon and Morel, 1983), modelling of light penetration and thermodynamics of the upper ocean (Zaneveld *et al.*, 1981; Lewis *et al.*, 1983; Kirk, 1988) the assessment of primary production by remote sensing (Platt and Sathyendranath, 1988), and the interpretation of *in situ* optical measurements, for example, those obtained with transmissometers (Siegel *et al.*, 1989). Each of the substances involved can, in principle, contribute independently to the optical properties of sea water, according to their concentration and their absorption and scattering characteristics. Therefore, to be able to distinguish the effect of one component on a particular optical property (*e.g.*, the effect of phytoplankton on ocean colour), it is necessary to be able to account for the contribution of all the others.

The optical properties of sea water are generally partitioned into contributions from pure water, phytoplankton, yellow substances (dissolved organic material), and inorganic sediments (*e.g.*, Jerlov 1976; Kirk, 1983). Furthermore, it is commonly considered that phytoplankton and their derived products are the main components determining the optical properties of sea water, particularly in deep-ocean waters, and also in coastal waters that are not significantly affected by terrigenous inputs or by the resuspension of sediments. Thus, phytoplankton and their derived products are believed to be the dominant contributors to the absorption and scattering characteristics of more than 98% of the world ocean waters (Morel, 1988). For these waters (known as Case 1 waters) current bio-optical models use phytoplankton pigment concentration as the master variable through which most of the inherent optical properties are estimated (*e.g.*, Morel and Prieur, 1977; Gordon *et al.*, 1988; Morel, 1988; Sathyendranath and Platt, 1988).

In spite of the relative success of such models in reproducing optical properpetics of sea water (for example, the irradiance reflectance or ocean colour) using only phytoplankton pigment concentration as the independent variable, some problems remain. In this thesis, I examine the independent role of non-chlorophyllous particles on the scattering properties of sea water, with particular reference to heterotrophic bacteria and sub-micrometer detrital particles.

Heterotrophic bacteria are microorganisms present in all marine environments, in number concentrations 1–2 orders of magnitude higher than phytoplankton; however their influence on the light field in the ocean has been little studied. They are small (typical diameter of ~ 0.5 μm), compared to the other organisms comprising the plankton; nevertheless they can make a significant contribution to the total planktonic biomass (in units of carbon), particularly in oligotrophic waters (Cho and Azam, 1990). Studies of their absorption and scattering characteristics have been carried out on cultures (Yentsch, 1962; Kopelevich *et al.*, 1987; Morel and Ahn, 1990; Stramski and Kiefer, 1990). These studies suggest that heterotrophic bacteria could contribute significantly to the scattering of light in the field. However, no direct evaluations of their contribution to the optical properties of sea water have yet been made.

On the other hand, attempts to recover the total backscattering coefficient as the sum of contributions from pure water, phytoplankton, and other components present in sea water have failed (Morel and Ahn, 1991; Stramski and Kiefer, 1991). In other words, from what is presently known about the optical properties of these substances, and their concentrations in natural waters, it is not possible to account for the amount of light that is backscattered in the ocean. It has been shown, however, that microorganisms can account for most of the total particle scattering

(Morel and Ahn, 1991; Stramski and Kiefer, 1991), and that phytoplankton are responsible for most of the particle absorption. This poses a problem: what is the missing component that contributes significantly to the backscattering, and yet does not modify absorption or total scattering coefficients?

Early models of light scattering by marine particles (Gordon and Brown, 1973; Brown and Gordon, 1973, 1974) suggested that very small, organic particles (≤ 1 μm) could be responsible for most of the backscattering in the ocean. Heterotrophic bacteria can be considered to be part of this component, but they do not constitute the whole. Recent theoretical studies indicate that particles other than heterotrophic bacteria should be considered to account for most of the backscattering (Morel and Ahn, 1991; Stramski and Kiefer, 1991). The presence of extremely small, detrital particles in large concentrations has recently been reported (Koike *et al.*, 1990; Longhurst *et al.*, 1991). These sub-micrometer, detrital particles could indeed account for the required backscattering, without contributing significantly to the total scattering and absorption. However, nothing is yet known about their optical properties, nor whether they are present in large concentrations in most of the world's ocean. Paradoxically, it would be the light backscattered by these small detrital particles that can be remotely sensed, giving information about the amount of phytoplankton present in the surface layers of the ocean.

On the other hand, the backscattering coefficient is presently modelled as a function of phytoplankton pigment concentration (Gordon *et al.*, 1988; Morel, 1988; Sathyendranath and Platt, 1988), through the product of the backscattering ratio (ratio of the backscattering coefficient to the total scattering coefficient) and the total scattering coefficient. While the latter has been shown to covary with pigments (Gordon and Morel, 1983), the former has been little studied. In current bio-optical models, the backscattering ratio is assumed to be constant (Sathyendranath and Platt, 1988) or to covary inversely with phytoplankton pigment concentration (Gordon *et al.* 1988; Morel, 1988).

In this thesis, I use the theory of light scattering (Mie theory; Mie, 1908) in combination with detailed *in situ* data of bacterial size and abundance to estimate the contribution of heterotrophic bacteria to the scattering of light in natural waters. I also use Mie theory to study the backscattering ratio for particle suspensions which include sub-micrometer particles.

The main objectives of this thesis are:

1) to determine the relative contribution of heterotrophic bacteria to light scattering in the ocean, and its relation to the amount of phytoplankton present in the water, and

2) to examine the role of sub-micrometer particles in determining the backscattering ratio of the total particle suspension, and its relation to the phytoplankton pigment concentration.

In Chapter 1, the Mie solutions for the problem of estimating scattering by polydispersions are presented, and examined for the particular case of estimating scattering by heterotrophic bacteria in the ocean. The suitability of using the much simpler approximations of van de Hulst is also examined; these approximations have been previously used (Morel and Ahn, 1991; 1992; Stramski and Kiefer, 1990) to deduce the refractive index of bacteria and to estimate their contribution to the absorption and scattering properties of sea water. The definitions of the optical properties and parameters used throughout the text are also given.

In Chapter 2, two simple approximations for the bacterial scattering coefficient are derived. The first one is for bacteria with a normal size distribution and the second one is for bacteria with a gamma size distribution. Both distributions are shown to be good representations of natural bacterial assemblages.

In Chapter 3, the optical properties of natural assemblages of heterotrophic bacteria and the bacterial contribution to the light scattering of sea water are estimated by applying Mie theory to field data on bacterial size and abundance. The estimates are made for three regions that contain different phytoplankton pigment concentrations. The utility of using pigment data to estimate bacterial scattering is also evaluated.

In Chapter 4, Mie theory is used to study the backscattering ratio due to particles in the ocean that obey a Junge-type distribution. Its sources of variation due to changes in the refractive index, wavelength, and the shape of the particle size distribution are examined. An explanation is given to why the backscattering ratio (and the backscattering coefficient) could covary with phytoplankton pigment concentration, although most of the backscattering would be due to sub-micrometer detrital particles and not phytoplankton.

Finally, a general discussion and the main conclusions of this thesis are given.

CHAPTER 1

Light Scattering by Polydispersions of Marine Heterotrophic Bacteria: Computations using Mie Theory and the van de Hulst Approximations

1.1 Introduction

The role of heterotrophic bacteria in radiative transfer in the ocean has been little studied. The common practice in marine optics has been to partition the optical properties of sea water into contributions from pure water, phytoplankton, yellow substances, and inorganic sediments (*e.g.*, Jerlov, 1976; Kirk, 1983), and therefore to ignore any independent contribution from non-chlorophyllous cells. Under this scheme, phytoplankton are considered to be the main component influencing the optical properties of ocean waters (Gordon and Morel, 1983).

Theories of light scattering have been used to account for the optical properties of biological particles (*e.g.*, Petukhov, 1965; Koch, 1968; Bryant *et al.*, 1969), as well as of suspended (organic and inorganic) particles in the ocean (Gordon and Brown, 1972; Brown and Gordon, 1973, 1974; Morel, 1973). With the assumption that the particles are spherical, Mie theory (Mie, 1908) and the simpler approximations of van de Hulst (1957) have been used for phytoplankton (Morel and Bricaud, 1981*a*, *b*, 1986; Bricaud and Morel, 1986), including autotrophic bacteria (Stramski and Morel, 1990), for marine heterotrophic bacteria (Morel and Ahn, 1990; Stramski and Kiefer, 1990), and more recently for heterotrophic nanoflagellates and ciliates (Morel and Ahn, 1991). These theories provide estimates of optical properties of the cells, given information only on their size and refractive index.

The coccoid shape, random orientation, and simple cellular structure of most free-living marine bacteria suggest that as a first approximation, bacteria may be assumed to be spherical and homogeneous particles. For such particles, Mie theory of scattering (Mie, 1908) gives exact solutions, provided that the refractive index of the particles is known. In this chapter, I examine the Mie solutions to the problem of estimating scattering by polydispersions of marine heterotrophic bacteria for the range of refractive indices that have been previously reported (Morel and Ahn, 1990; Stramski and Kiefer, 1990). I also examine the suitability of using the much simpler approximations of van de Hulst (1957), and show that for the size range of marine bacteria observed in the field, the van de Hulst approximations lead to significant errors in the estimation of their optical properties. I start by outlining the definitions of the optical properties and parameters to be used throughout the text.

1.2 Inherent Optical Properties of an Aquatic System

The absorption and scattering properties of an aquatic system, composed of pure water plus other substances in solution and in suspension, can be specified in terms of the total absorption coefficient a, the total scattering coefficient b, the total attenuation coefficient c, and the total volume scattering function $\beta(\theta)$. These properties are referred to as the inherent optical properties (Preisendorfer, 1961), since their magnitudes depend only on the substances comprising the system and are independent of the geometry of the incident radiant field.

The inherent optical properties (all with dimensions [L^{-1}]) are defined for an infinitesimally thin layer of the system illuminated by a monochromatic collimated beam normal to the layer (Fig. 1.1). Let ϕ_o be the incident radiant flux, $d\phi_a$ and $d\phi_b$ the absorbed and scattered fluxes, respectively, $d\phi(\theta)$ the flux scattered into an element of solid angle $d\omega$ oriented at angle θ to the direction of the incident beam, and dr the thickness of the layer. Then we have (*cf.* Kirk, 1983)

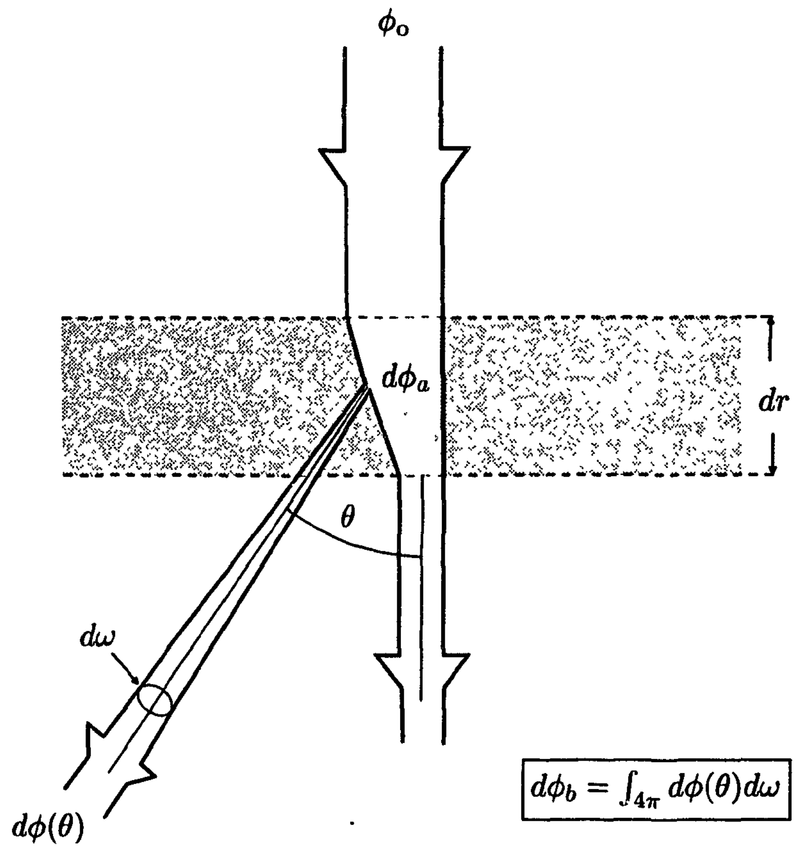

FIGURE 1.1. Geometry used to define inherent optical properties.

$$a = -\frac{1}{\phi_o}\frac{d\phi_a}{dr} \; ; \tag{1.1a}$$

$$b = -\frac{1}{\phi_o}\frac{d\phi_b}{dr} \; ; \tag{1.1b}$$

$$c = a + b \; ; \tag{1.1c}$$

and

$$\beta(\theta) = \frac{1}{\phi_o}\frac{d^2\phi(\theta)}{d\omega dr} \; . \tag{1.1d}$$

The integral of equation (1.1d) over all directions yields the total scattering coefficient. For scattering with rotational symmetry,

$$b = 2\pi \int_0^{\pi} \beta(\theta) \sin\theta d\theta \; . \tag{1.2}$$

For many optical problems (e.g., theory of ocean colour), it is necessary to distinguish between light that is scattered into the forward and the backward directions. The total backscattering coefficient (or total backward scattering coefficient) b_b is obtained by integrating the total volume scattering function over the backward hemisphere ($\pi/2 \leq \theta \leq \pi$):

$$b_b = 2\pi \int_{\pi/2}^{\pi} \beta(\theta) \sin\theta d\theta \; . \tag{1.3}$$

The total backscattering ratio $\tilde{b}_b$ is defined as the ratio of the total backscattering coefficient to the total scattering coefficient:

$$\tilde{b}_b = \frac{b_b}{b} \; . \tag{1.4}$$

1.3 Optical Properties of a Single Particle

When a single particle is illuminated by a monochromatic, collimated beam, a certain fraction of the incident radiant flux is absorbed or scattered (or both) from the beam. The efficiency factors (dimensionless) for absorption Q_a, scattering Q_b, and attenuation Q_c are defined as the ratios of the absorbed, scattered, and attenuated (absorbed + scattered) fluxes, respectively, to the radiant flux incident onto the geometrical cross-section of the particle normal to the incident beam (van de Hulst, 1957).

The refractive index of the particle relative to the surrounding medium (water) is specified by a complex number

$$m = n - in' , \tag{1.5}$$

where the real part n corresponds to the ratio of the phase velocity of light in the medium to the phase velocity of light inside the particle, and the imaginary part n' describes the decrease in electric field strength or the decay of the energy flux; n' is related to a', the absorption coefficient of the material of which the particle is made, according to

$$n' = \frac{a'\lambda}{4\pi m_w} , \tag{1.6}$$

where λ is the wavelength of light in vacuum and m_w is the refractive index of the medium (water). In the visible range (400–700 nm), the imaginary part of m_w is less than 10^{-7} and can therefore be neglected. With this approximation, m_w can be replaced by $n_w = 1.34$ (Jerlov, 1976), the real part of the refractive index of water in the visible range.

1.4 Mie Scattering

The optical characteristics of an optically homogeneous spherical particle can be determined precisely using Mie theory (Mie, 1908; van de Hulst, 1957). The relevant dimensionless parameters involved in the calculations are m, the complex refractive index of the particle relative to that of the surrounding medium, and x, the size of the particle scaled to the wavelength of light in the medium according to

$$x = \frac{\pi D n_w}{\lambda} , \tag{1.7}$$

where D is the diameter of the particle, n_w is the real part of the refractive index of water, and λ is the wavelength of light in vacuum.

The Mie solutions are expressed in terms of the complex coefficients (van de Hulst, 1957)

$$a_k(m,x) = \frac{\psi_k(x)\psi_k'(y) - m\psi_k(y)\psi_k'(x)}{\zeta_k(x)\psi_k'(y) - m\psi_k(y)\zeta_k'(x)} ; \tag{1.8a}$$

and

$$b_k(m,x) = \frac{m\psi_k(x)\psi_k'(y) - \psi_k(y)\psi_k'(x)}{m\zeta_k(x)\psi_k'(y) - \psi_k(y)\zeta_k'(x)} , \tag{1.8b}$$

where $y = mx$, ψ_k and ζ_k are the Riccati-Bessel functions, and the primes denote differentiation with respect to the argument (Appendix I). The efficiency factors for attenuation $Q_c(m,x)$, scattering $Q_b(m,x)$, and absorption $Q_a(m,x)$ are given by

$$Q_c(m,x) = \frac{2}{x^2}\sum_{k=1}^{\infty}(2k+1)Re(a_k + b_k) ; \tag{1.9a}$$

$$Q_b(m,x) = \frac{2}{x^2}\sum_{k=1}^{\infty}(2k+1)(|a_k|^2 + |b_k|^2) ; \tag{1.9b}$$

and

$$Q_a(m,x) = Q_c(m,x) - Q_b(m,x) \ . \tag{1.9c}$$

The angular distribution of the scattered light is specified by the dimensionless angular intensity parameters

$$\begin{aligned} i_1(\theta,m,x) &= |S_1(\theta,m,x)|^2 \\ &= \left| \sum_{k=1}^{\infty} \frac{2k+1}{k(k+1)} \left[a_k \pi_k(\mu) + b_k \tau_k(\mu) \right] \right|^2 \end{aligned} \tag{1.10a}$$

and

$$\begin{aligned} i_2(\theta,m,x) &= |S_2(\theta,m,x)|^2 \\ &= \left| \sum_{k=1}^{\infty} \frac{2k+1}{k(k+1)} \left[a_k \tau_k(\mu) + b_k \pi_k(\mu) \right] \right|^2 \ , \end{aligned} \tag{1.10b}$$

where $S_1(\theta,m,x)$ and $S_2(\theta,m,x)$ are the complex amplitude functions for the perpendicular and the parallel components of the electric field vector, $\pi_k(\mu) = dP_k(\mu)/d\mu$ and $\tau(\mu) = \mu dP_k(\mu)/d\mu - (1-\mu^2)d^2P_k(\mu)/d\mu^2$ are angular functions where $P_k(\mu)$ is the Legendre polynomial of order k and $\mu = \cos\theta$, and θ is the scattering angle.

The efficiency factor for backscattering, Q_{b_b}, can be computed directly from the Mie coefficients (Chýlek, 1973), or alternatively, by integrating numerically the angular intensity parameters over the backward hemisphere:

$$Q_{b_b}(m,x) = x^{-2} \int_{\pi/2}^{\pi} \left[i_1(\theta,m,x) + i_2(\theta,m,x) \right] \sin\theta d\theta \ . \tag{1.11}$$

Note that this expression for Q_{b_b} differs by a factor of two from that in Bricaud and Morel (1986), and in Morel and Bricaud (1986).

Figures 1.2a and 1.2b show the variation in Q_b (=Q_c when $n' = 0$) and Q_a as a function of x for different values of n and n', respectively. Figures 1.2c and 1.2d show the variation of Q_{b_b} and b_b with x for different values of n. Computations were carried out with code according to Bohren and Huffman (1983), which does not give Q_{b_b} directly but allows it to be computed from the intensity functions. The scattering curve (Fig. 1.2a) shows that Q_b increases from 0 (=$\lim_{x\to 0} Q_b$) to a maximum value of > 3, and then undergoes a damped oscillation about the limiting value $Q_b = 2$ (when $n' = 0$). The maximum occurs at $\rho = 2x(n-1)$, where ρ is the difference between the phase shift which the central ray experiences upon traversing the particle diameter and that obtained in the absence of the particle (*i.e.*, the phase lag). The efficiency factor for absorption Q_a (Fig. 1.2b) increases monotonically to its limiting value $Q_a = 1$. For backscattering (Fig. 1.2c), the efficiency factor Q_{b_b} has a first maximum at $x = 2.24$, and then increases with small oscillations to its limiting value (proportional to the amount of radiation reflected by the particle, and therefore to Fresnel's factor $|n-1|^2/|n+2|^2$). The backscattering ratio $\tilde{b}_b = Q_{b_b}/Q_b$ (Fig. 1.2d) decreases from its limiting value 0.5, has a first small minimum (first maximum in the backscattering curve), and then decreases again to a broad minimum, coincident with the first maximum in Q_b.

In field data from the Western North Atlantic (see Chapter 3), the equivalent spherical diameter D for bacteria (defined as the diameter of a sphere having a cross-sectional area equal to the projected area of the particle) varies from about 0.2 to 1.4 μm. For wavelengths in the visible range (400 to 700 nm), the corresponding size parameter x will vary between 1.2 and 14.7. To my knowledge, no direct measurements of the refractive indices of marine bacteria have been made. Morel and Ahn (1990) indirectly estimated the real part n to be around 1.05, with a range from 1.04 to 1.06, based on measurements made on marine bacteria in culture, and using the anomalous diffraction approximation (van de Hulst, 1957). Using a similar approach, Stramski and Kiefer (1990) estimated n to be between 1.04 and

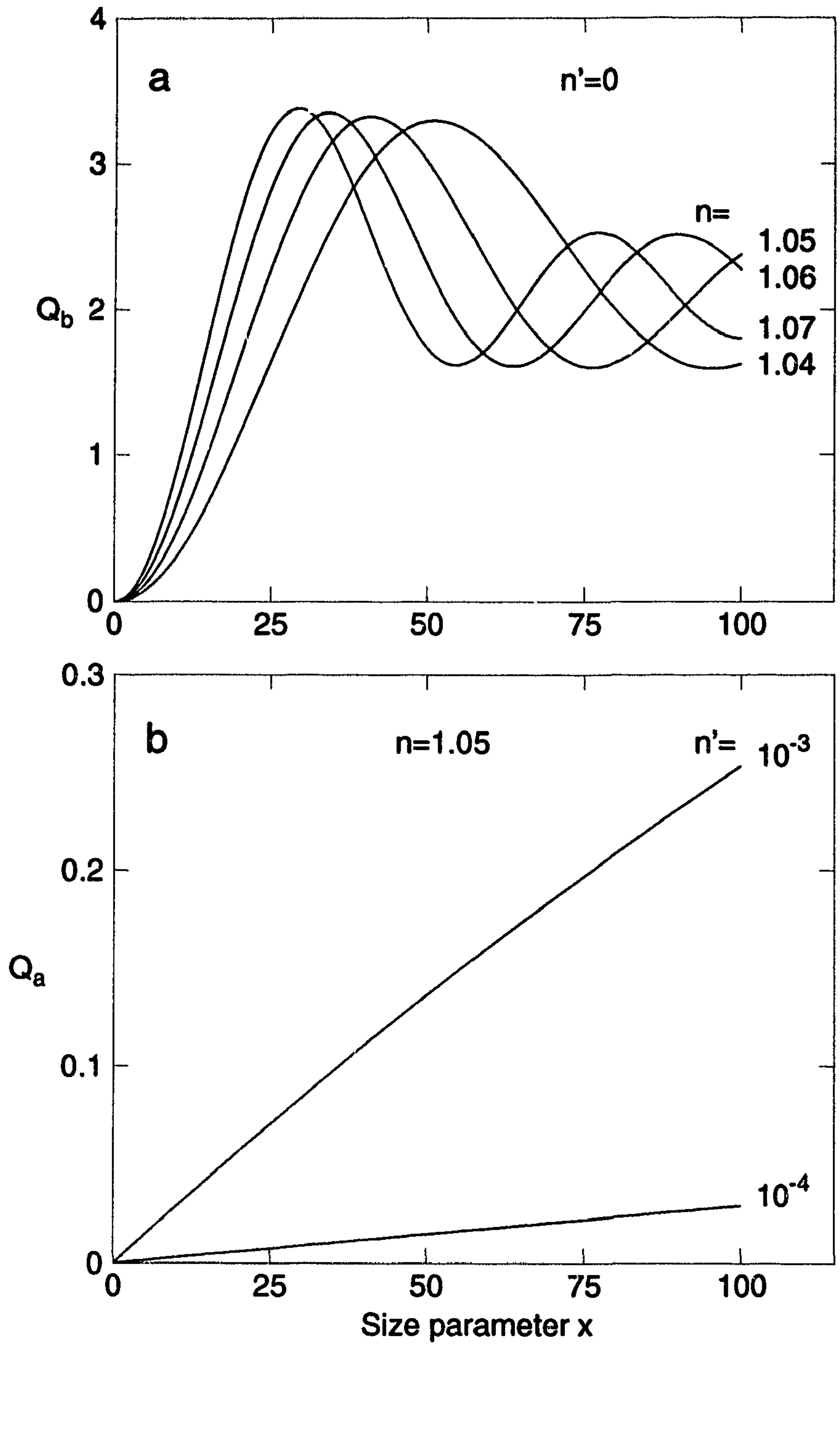

FIGURE 1.2. Efficiency factors for (*a*) scattering (Q_b), (*b*) absorption (Q_a), and (*c*) backscattering (Q_{b_b}) as a function of the size parameter x; (*d*) the backscattering ratio ($\tilde{b}_b$) as a function of x.

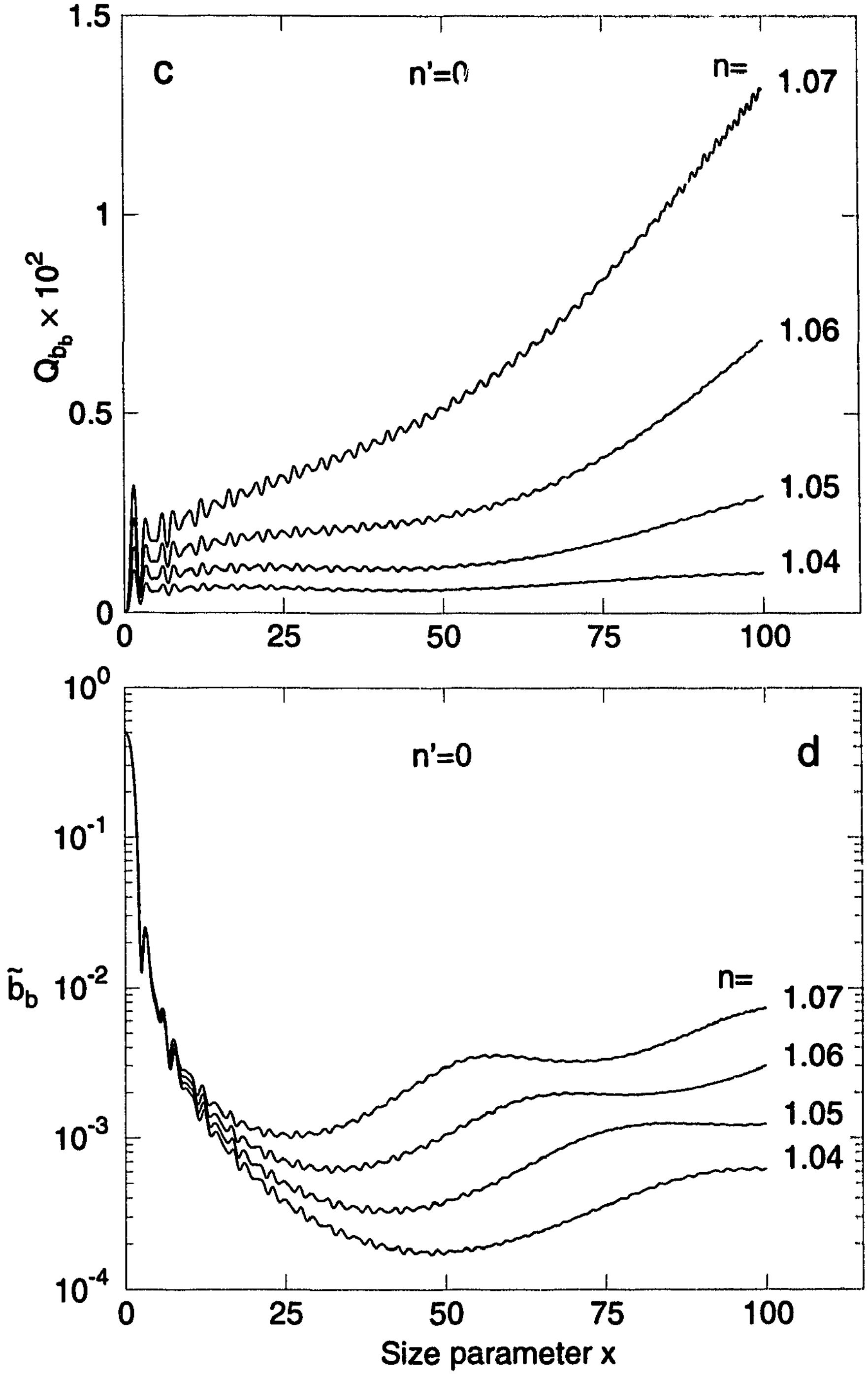

FIGURE 1.2. Continuation.

1.07, but they computed the complete Mie solutions instead of using the anomalous diffraction approximation. Values in the literature for refractive indices of non-marine bacteria fall in the range 1.03 to 1.06 relative to water (Bateman *et al.*, 1966).

The n' values deduced for marine bacteria, less than 2×10^{-3} according to Morel and Ahn (1990) and of the order of 10^{-4} according to Stramski and Kiefer (1990) showed some spectral dependance, with a maximum in the blue region of the visible spectrum. With these low values for n', the influence of absorption on Q_b or Q_{b_b} (Fig. 1.3) is minimal. (Note, however, that this does not mean that the contribution of bacteria to the total absorption coefficient is necessarily insignificant.) On the basis of these results and observations, I take $(1.05 - 0.0001i)$ to be the typical complex value for m representative of marine bacteria but examine the theoretical results for the whole range of n reported in the literature to evaluate the uncertainty in the results. With this value for m, $D \approx 0.5$ μm, and $\lambda = 440$ nm, $Q_b \approx 0.2$, $Q_a \approx 0.002$, $Q_{b_b} \approx 0.001$, and $\tilde{b}_b \approx 0.005$. Note that for the range of sizes and refractive indices representative of bacteria, the size parameter range lies below the first maximum in the scattering curve (Figs. 1.2*a* and 1.3).

1.5 Influence of Bacteria on the Optical Properties of an Aquatic System

The influence of bacteria, considered as a collection of particles, on the absorption and scattering properties of an aquatic system can be specified through their contribution to the inherent optical properties of the system (a, b, c, b_b, and $\beta(\theta)$). With respect to size, two cases can be considered: one in which all the cells have the same diameter (monodispersion), and the other in which the cells differ in size (polydispersion).

1.5.1 Monodispersion. For a system containing N bacteria of the same size per unit volume, and assuming no multiple scattering, the partial contribution of bacteria to the total scattering coefficient is

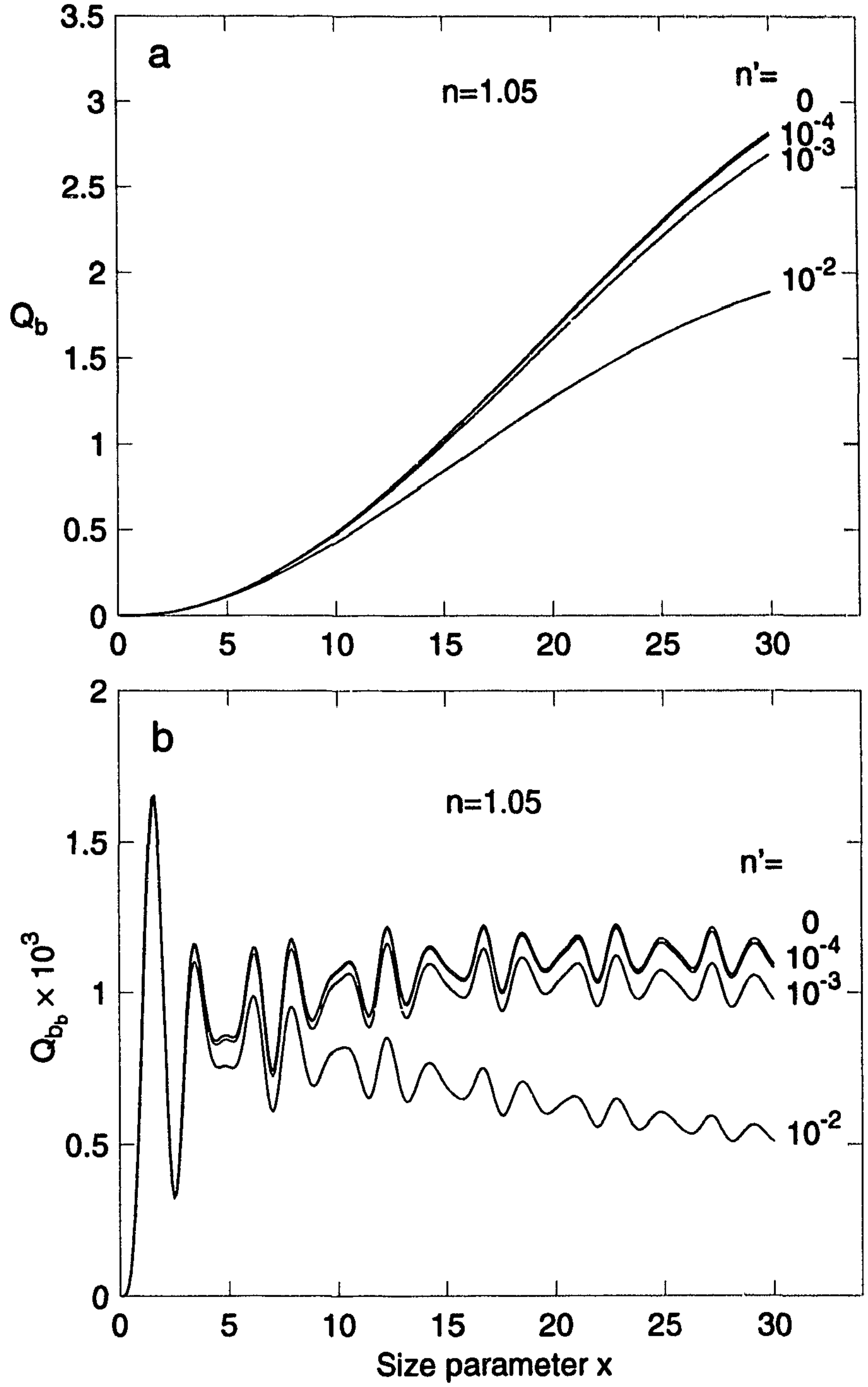

FIGURE 1.3. Influence of n', the imaginary part of the refractive index, on (a) Q_b and (b) Q_{b_b} when $n = 1.05$.

$$b_h = N Q_b s \ , \tag{1.12}$$

where s is the geometrical cross-section of the particle and the subscript h specifies that the scattering is due to heterotrophic bacteria. The contribution of bacteria to the total absorption, total attenuation, and total backscattering can also be specified in terms of coefficients a_h, c_h, and b_{bh} respectively, by replacing Q_b by Q_a, Q_c, and Q_{b_b} in equation (1.12). The bacterial contribution to the total volume scattering function $\beta(\theta)$ for unpolarized light is given by

$$\beta_h(\theta) = \frac{\lambda^2 N}{8\,\pi^2\,n_w^2}[i_1(\theta,x) + i_2(\theta,x)] \ , \tag{1.13}$$

where $i_1(\theta,x)$ and $i_2(\theta,x)$ are the angular intensity parameters given by equations (1.10a) and (1.10b).

1.5.2 Polydispersion. For bacteria with a size distribution function $F(D) = Nf(D)$, where D is the diameter and $f(D)$ is the probability density function ($\int_0^\infty f(D)dD = 1$), we have (*cf.* van de Hulst, 1957)

$$j_h = \frac{\lambda^2\,N}{4\,\pi\,n_w^2}\int_0^\infty Q_j(x)x^2 f(x)dx \ , \tag{1.14}$$

where j can mean a, b, c, or b_b according to the particular case, and for unpolarized light

$$\beta_h(\theta) = \frac{\lambda^2\,N}{8\,\pi^2\,n_w^2}\int_0^\infty [i_1(\theta,x) + i_2(\theta,x)]\ f(x)\ dx \ . \tag{1.15}$$

The function $f(x)$ is obtained directly from $f(D)$ by change of variable using equation (1.7).

An effective efficiency factor $\bar{Q}_j$ can also be defined for the entire population (van de Hulst, 1957),

$$\bar{Q}_j = \frac{\int_0^\infty Q_j(x)x^2 f(x)dx}{\int_0^\infty x^2 f(x)dx} , \tag{1.16}$$

which corresponds to the ratio of the total optical cross-section for $j = a, b, c$, or b_b, to the total geometrical cross-section.

1.6 The van de Hulst Approximations

For homogeneous spherical particles with refractive index close to 1 and $x \gg 1$, the efficiency factor Q_c can be computed more easily using the anomalous diffraction approximation (van de Hulst, 1957):

$$\begin{aligned} Q_c(\rho) &= 2 - 4e^{-\rho \tan\xi} \left(\frac{\cos\xi}{\rho}\right) \sin(\rho - \xi) \\ &+ 4\left(\frac{\cos\xi}{\rho}\right)^2 \left[\cos(2\xi) - e^{-\rho\tan\xi}\cos(\rho - 2\xi)\right] , \end{aligned} \tag{1.17}$$

where $\rho = 2x(n-1)$ and $\tan\xi = n'/(n-1)$. In addition, van de Hulst (1957) derived an expression for Q_a, valid under the same conditions:

$$Q_a(\rho') = 1 + 2\,\frac{e^{-\rho'}}{\rho'} + 2\,\frac{e^{-\rho'} - 1}{\rho'^2} , \tag{1.18}$$

where $\rho' = 4xn'$. The efficiency factor Q_b is then given by the difference between Q_c and Q_a. However, under this scheme, no expressions are available either for Q_{b_b} or for the angular intensity functions. Note that the expression for Q_a given in equation (1.18) is identical to the solution of Duysens (1956). Both Duysens (1956) and van de Hulst (1957) make the same approximations in deriving the expression for Q_a (for example, no refraction at the interface between the particle and the medium).

For the size parameter range representative of bacteria (~1 to 15) the condition $x \gg 1$ is not satisfied everywhere. To test the validity of the van de Hulst expressions over the ranges of x and m typical for bacteria, the exact Mie solutions for Q_a and Q_c were calculated and compared with the approximate results according to equations (1.17) and (1.18). For n between 1.04 and 1.07 and for x between 1 and 15, the error for Q_a was found to be less than 15% for $n' \leq 10^{-2}$ (Fig. 1.4), while the error in Q_b can exceed 100% (Fig. 1.5; see also Moore *et al.*, 1968). I also examined the error in the case of polydisperse suspensions. For a given $\bar{x}$, the standard deviation (σ_x) in the gamma distribution was varied. The results for $m = 1.05$ are shown in Figure 1.6. It is clear that the error in $\bar{Q}_b$ can exceed 100%, depending mainly on $\bar{x}$. This error increases rapidly with decreasing $\bar{x}$.

Morel and Ahn (1990) and Stramski and Kiefer (1990) have relied on the van de Hulst approximation for Q_a to evaluate n', and Morel and Ahn (1990) used the anomalous diffraction approximation for Q_c to estimate n. I have tried to evaluate whether the corresponding errors are within reasonable limits when applied to bacteria.

According to this method, which was originally described by Bricaud and Morel (1986) and later modified by Stramski *et al.* (1988), the imaginary part of the refractive index n' is first determined at each wavelength of the spectrum by an iterative process: the computed $\bar{Q}_a(\rho')$ obtained from equations (1.16) and (1.18) is matched with a laboratory-determined value of $\bar{Q}_a$. The experimental $\bar{Q}_a$ at a given wavelength is in turn obtained from measurements of the bacterial absorption coefficient a_h and the size distribution $f(D)$, according to

$$\bar{Q}_a = \frac{4}{\pi} \frac{a_h}{N \int_0^\infty f(D)\, D^2\, dD} \,. \tag{1.19}$$

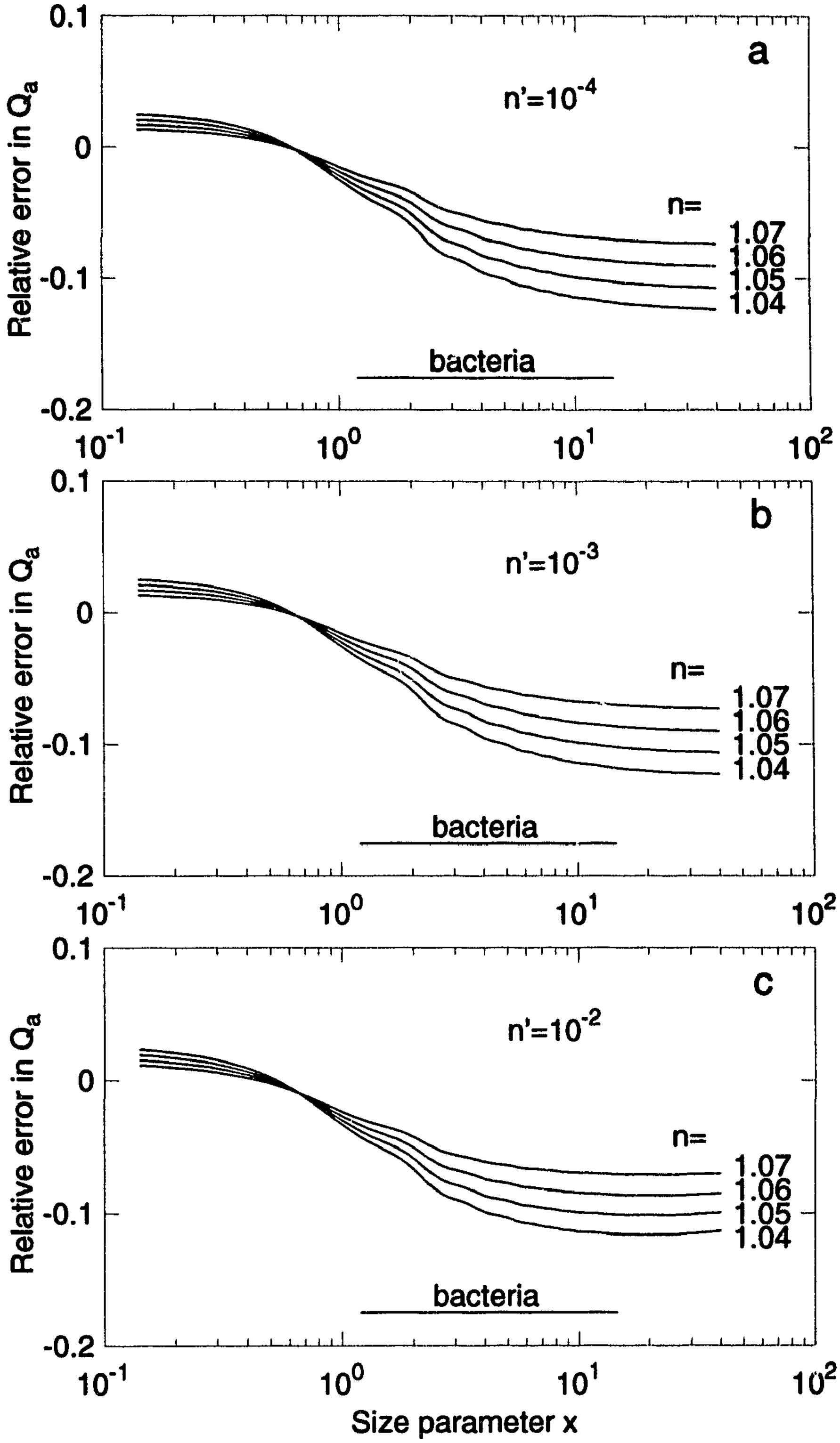

FIGURE 1.4. Relative error in computation of Q_a using the van the Hulst approximation, compared with the exact Mie solution for a homogeneous sphere, as a function of x, and for (a) $n' = 10^{-4}$, (b) $n' = 10^{-3}$, and (c) $n' = 10^{-2}$.

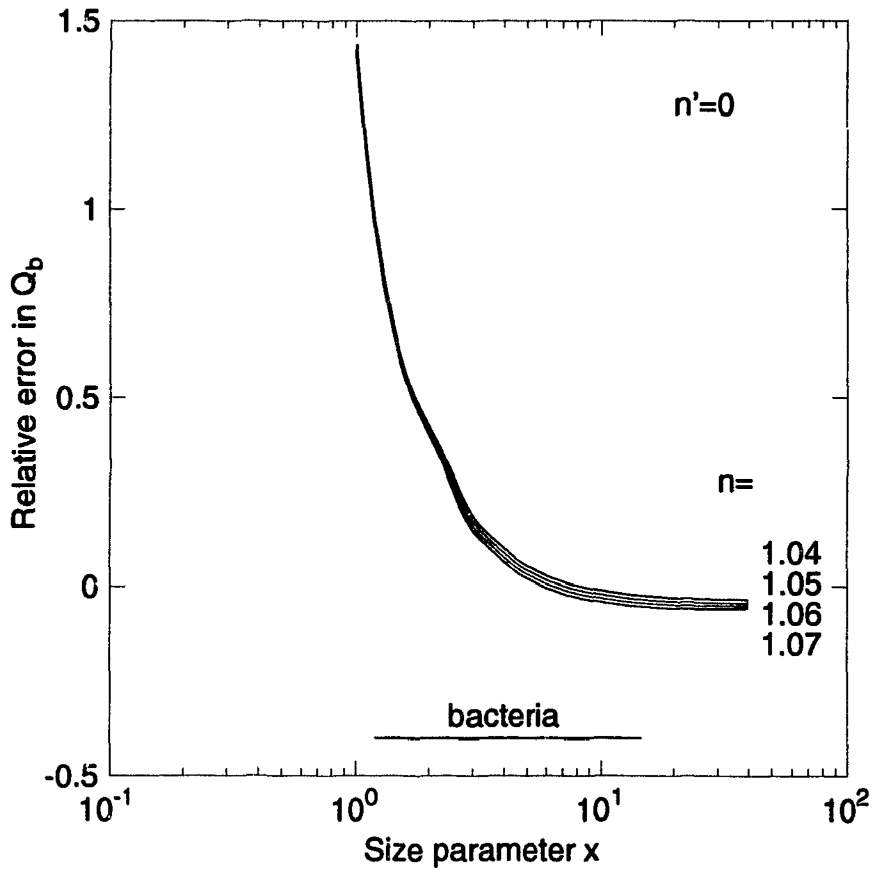

FIGURE 1.5. Relative error in computation of Q_b ($=Q_c$ when $n' = 0$) using the anomalous diffraction approximation of van de Hulst as a function of x for different values of n.

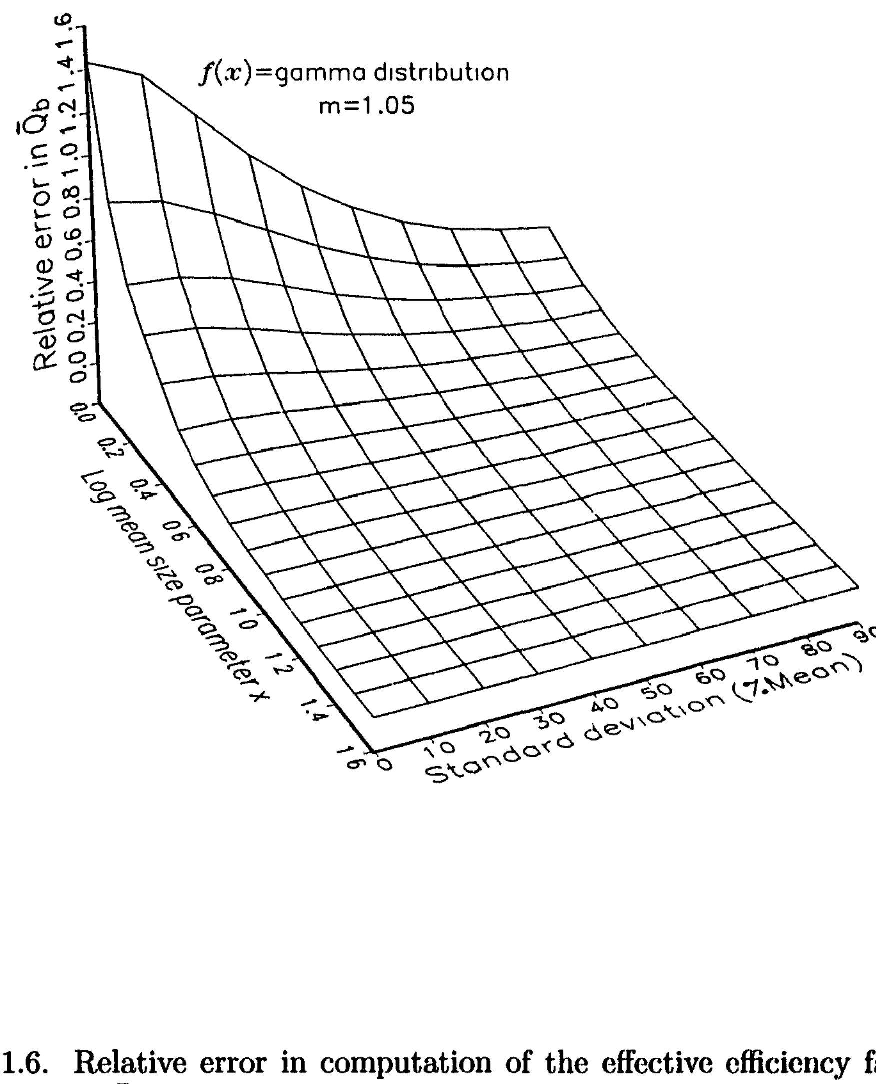

FIGURE 1.6. Relative error in computation of the effective efficiency factor $\bar{Q}_b$ ($=\bar{Q}_c$ when $n' = 0$) using the anomalous diffraction approximation as a function of the mean and the standard deviation of the size parameter of a polydispersion with a gamma size distribution and $m = 1.05$.

Compared with the exact Mie computations, I have established that this method will give n' values within 20% over the range in x and m representative of marine bacteria (Fig. 1.7).

The next step in the method, as modified by Stramski *et al.* (1988), is the determination of the real part of the refractive index by iteration. By varying n, a computed efficiency factor for attenuation $\bar{Q}_c(\rho)$ is made to match the corresponding experimental $\bar{Q}_c$ value. The computed $\bar{Q}_c$ values are obtained from equations (1.16) and (1.17), and the experimental values are obtained from an equation analogous to equation (1.19).

I estimated the error in n, as estimated using the anomalous diffraction approximation of van de Hulst, by the following iterative process. I varied n such that a $\hat{Q}_c$, computed using equation (1.17), was made to approach a Q_c obtained from Mie computation for a given n and x. The iteration was terminated when $|\hat{Q}_c/Q_c - 1| \leq 10^{-3}$. I took the n value used to compute Q_c as the initial guess to obtain $\hat{Q}_c$. The results for the relative error in $(n-1)$ as a function of n and x are shown in Figure 1.8.

For the low end in the size parameter range of interest here, the errors are significant. (Note that the size parameters for bacteria in the data of Morel and Ahn (1990) are in the higher end of the size range considered here, and consequently their analysis would be less affected by this type of error.) In the region where Q_c (or $\bar{Q}_c$) starts to oscillate (Fig. 1.9) the method of Stramski *et al.* (1988) does not give a unique solution for n, as was originally recognized by the authors (Stramski *et al.*, 1988). Furthermore, for many values of Q_c there is no solution for the iteration at all, because the Q_c (or $\bar{Q}_c$) values computed with the van the Hulst approximation never reach the Q_c (or $\bar{Q}_c$) values obtained from the Mie equations (Fig. 1.9).

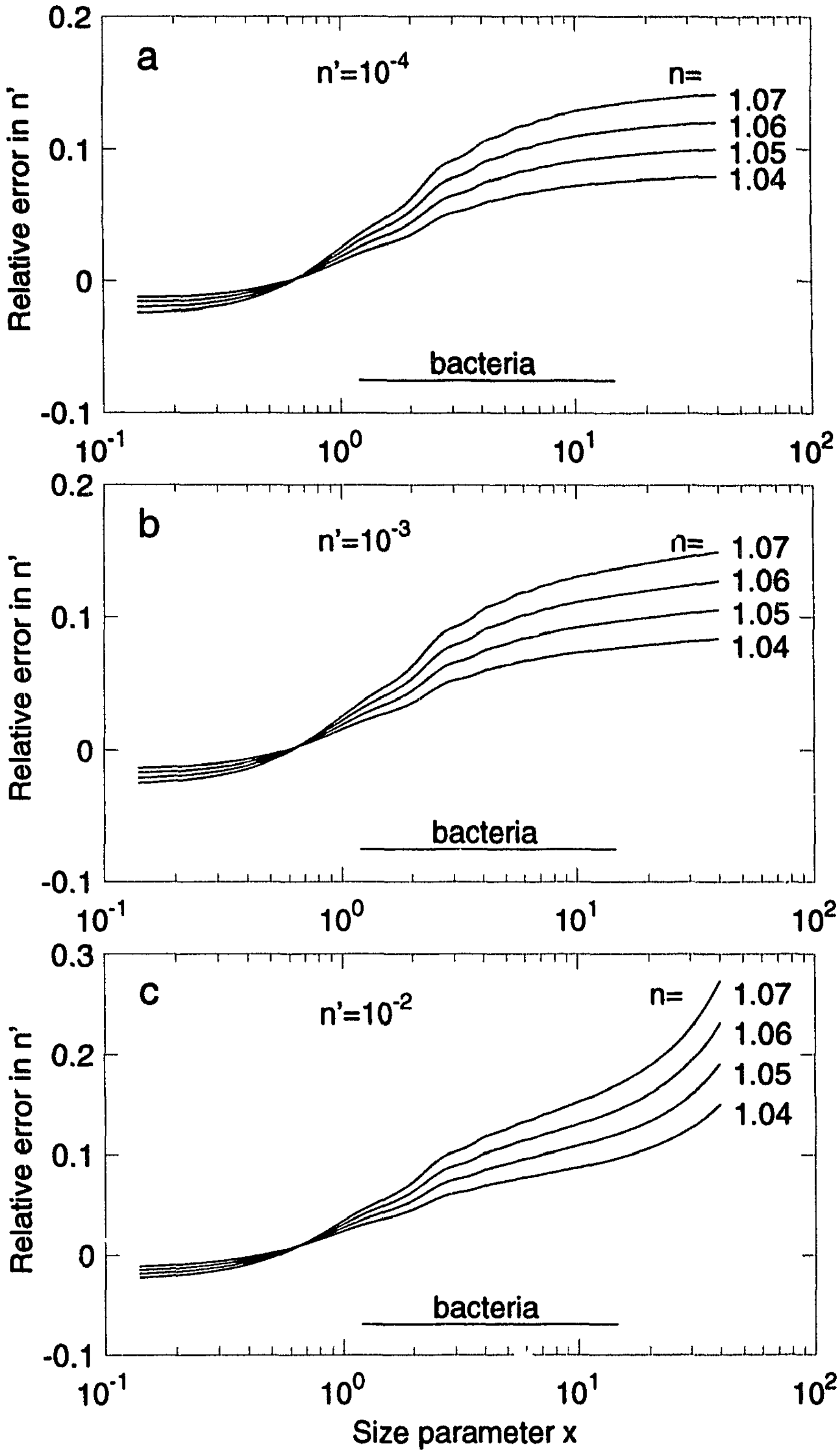

FIGURE 1.7. Relative error in computation of n' using the van the Hulst approximation, for different values of n and for $n' =$ (*a*) 10^{-4}, (*b*) 10^{-3}, and (*c*) 10^{-2}.

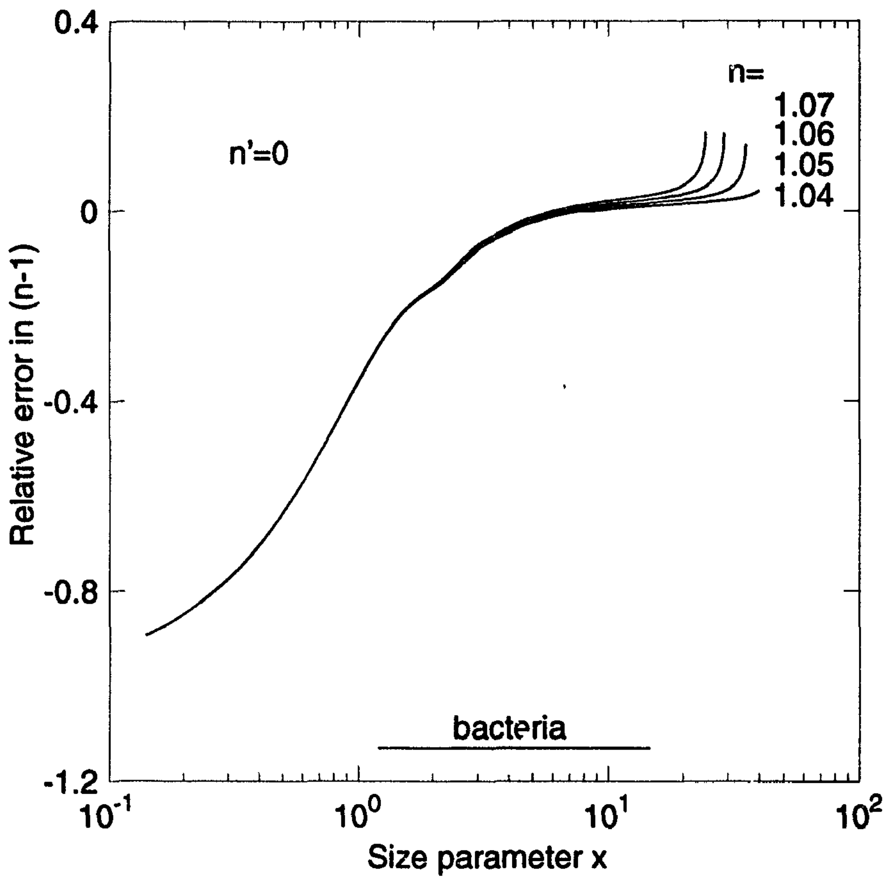

FIGURE 1.8. Relative error in computation of $n-1$ using the anomalous diffraction approximation as a function of x and for different values of n.

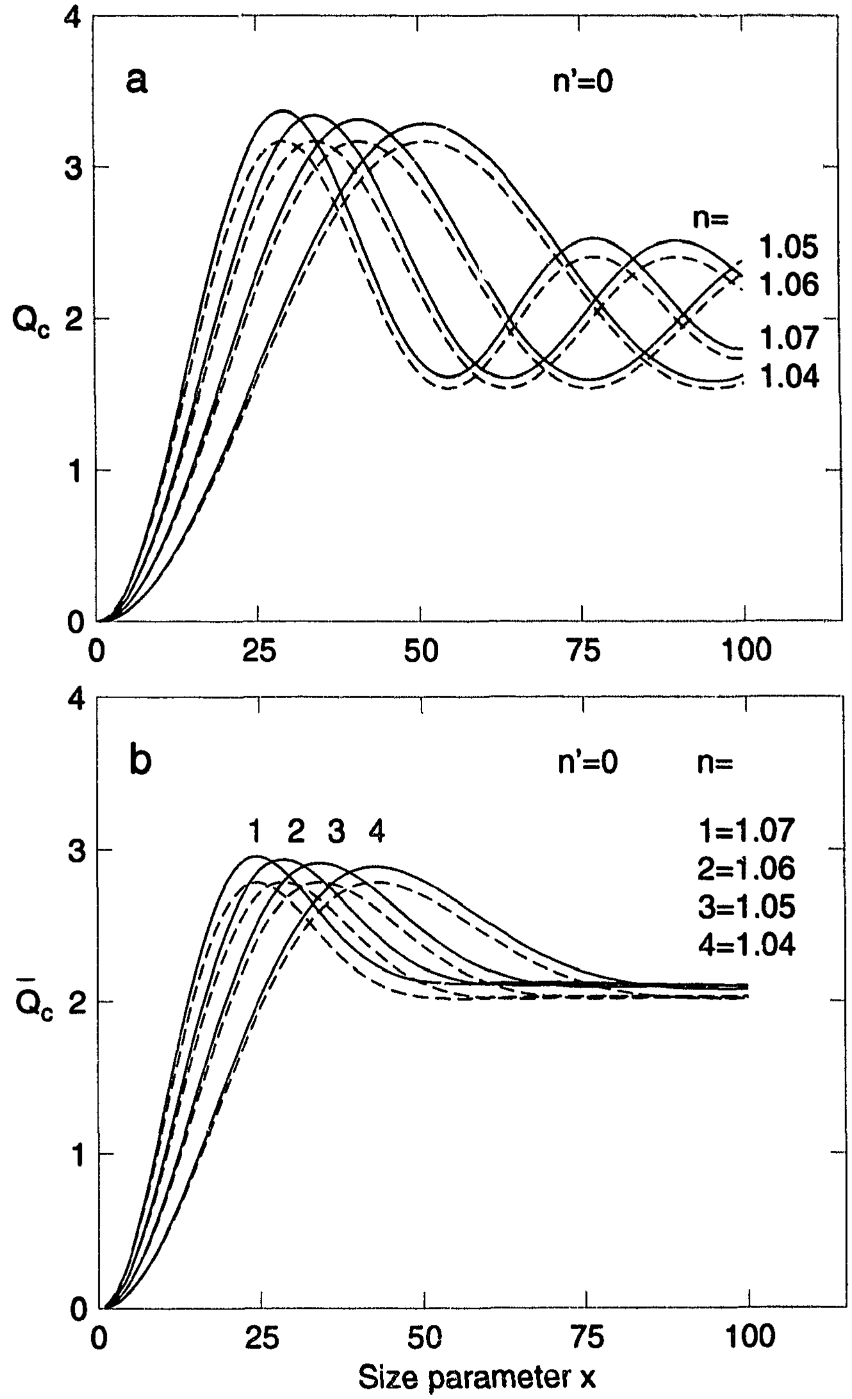

FIGURE 1.9. (*a*) Q_c as a function of x for a monodispersion with $m = 1.05$ obtained from Mie theory (solid line) and the anomalous diffaction approximation (dashed line), (*b*) as in (*a*) but for a polydispersion with a gamma size distribution with a standard deviation of 30% the mean of x. Note that for some values of x the Q_c values computed with the van the Hulst approximation do not reach the Q_c values computed from Mie theory.

1.7 Concluding Remarks

From a theoretical point of view, I have shown that the van de Hulst (1957) approximations cannot always be used to describe the scattering of light by natural bacterial assemblages, because their characteristic size-parameter range lies, in part, outside the range for which the approximation is valid. Modern computers allow the application of the more complete and strict Mie theory, which has been shown to explain well the experimental observations on light scattering by bacterial suspensions (*e.g.*, Petukhov, 1965; Shimizu and Ishimaru, 1978).

The application of Mie theory to estimate scattering by marine bacteria in natural waters will require information on their concentration, size distribution, and refractive index. The concentration and size distribution of natural bacterial assemblages can be measured directly, but it is still a time-consuming procedure. Particularly promising in this respect is the application of automated techniques such as flow cytometry (Robertson and Button, 1989; Frankel *et al.*, 1990), which allows the optical characterization and sizing of a large number of cells in a relatively short time.

The refractive index of marine bacteria has not yet been measured directly, but only deduced from optical measurements on laboratory cultures (Morel and Ahn, 1990; Stramski and Kiefer, 1990), an approach which in turn is subject to some error, as was shown here. Flow cytometry has also been used to derive the refractive index of marine particulates (Ackleson and Spinrad, 1988) and could be used in the case of marine bacteria. This approach, however, also relies *a priori* on the Mie theory.

CHAPTER 2

Simple Approximations for the Bacterial Scattering Coefficient

2.1 Introduction

The contribution of a polydispersion of N heterotrophic bacteria per unit volume, and with size distribution $F(x)$, to the total scattering coefficient b is given by (see equation 1.14 in Chapter 1)

$$b_h = \frac{\lambda^2 N}{4\pi n_w^2} \int_0^\infty Q_b(m,x)\, x^2 f(x) dx \ , \tag{2.1}$$

where λ is the wavelength of light in vacuum; n_w is the refractive index of the medium (water); Q_b is the efficiency factor for scattering; $f(x)$ is the probability density function, such that $F(x) = N f(x)$; m is the refractive index of the cells relative to the medium; and x is the size parameter ($x = \pi D n_w/\lambda$), which scales the diameter of the cells, D, to the wavelength of light in the medium. The subscript h indicates that the contribution is due to heterotrophic bacteria.

In the above equation, Q_b can be computed using Mie theory (assuming that the cells are spherical and optically homogeneous), but it is a complicated function of the arguments, involving Riccati-Bessel functions and their derivatives (*e.g.*, van de Hulst, 1957). Furthermore, given a size distribution $f(x)$, equation (2.1) will require numerical integration. Economy of computing time dictates a preference for analytic solutions when the results so obtained have the required accuracy. Computing efficiency could be crucial when the solutions are to be incorporated into other bio-optical models, for example, in the calculation of primary production from remotely sensed data (Platt and Sathyendranath, 1988). Furthermore, when the full size distribution is not available, a simple approximation is useful. Morel and Ahn (1990, 1991) gave simple formulae for the scattering and absorption coefficients due to bacteria, but their expressions are based on van de Hulst approximations and are applicable only to monodisperse populations. Here, I derive a more exact solution for polydisperse suspensions.

2.2 Approximation for $Q_b(x)$

The first step is to find a simple expression for $Q_b(x)$. For m between 1.04 and 1.07 and for $x \leq 30$, I found that the monotonic increase of Q_b with x (Fig. 2.1) can be empirically approximated by

$$Q_b(x) = \sum_{j=0}^{k} \alpha_j x^j \ , \tag{2.2}$$

where α_j are empirically-determined coefficients that depend only on m (Ulloa *et al.*, 1992). For $k = 5$, the relative error in Q_b is less than 7% over the size parameter range of interest. The coefficients α_j for different values of n and n' are given in Table 2.1. Similar approximations have recently been developed for the efficiency factors of water clouds (Chýlek *et al.*, 1992*a*, *b*; Damiano, 1992).

The next step is to select a function that fits the actual size distribution. Among the two-parameter distribution functions used to describe naturally occurring particles, the most common are the normal and the log-normal distributions. However, in the case of skewed distributions, the gamma distribution has also been shown to fit the experimental data well (Deirmendjian, 1969). In the next sections I give the solution for the normal and the gamma distributions.

2.3 Normal Distribution

For a population of bacteria with a normal distribution we have that

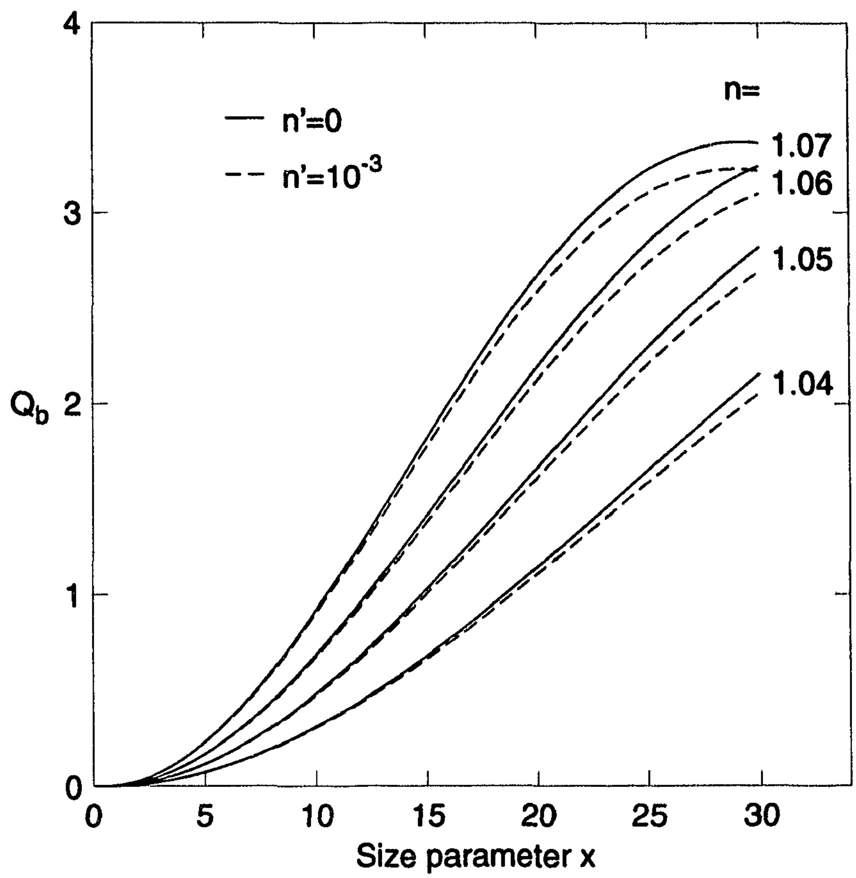

FIGURE 2.1. The variation of Q_b with x for different values of m when $x \leq 30$.

m	α_0	α_1	α_2	α_3	α_4	α_5
$1.04 - 0i$	2.1067×10^{-4}	-2.6768×10^{-3}	3.6311×10^{-3}	-1.4931×10^{-5}	-9.7510×10^{-7}	6.6087×10^{-9}
$1.04 - 0.0001i$	2.1278×10^{-4}	-2.6791×10^{-3}	3.6322×10^{-3}	-1.5613×10^{-5}	-9.6744×10^{-7}	6.6504×10^{-9}
$1.04 - 0.001i$	2.2358×10^{-4}	-2.6911×10^{-3}	3.6419×10^{-3}	-2.1541×10^{-5}	-9.0154×10^{-7}	7.0599×10^{-9}
$1.05 - 0i$	2.5404×10^{-4}	-4.1414×10^{-3}	5.7044×10^{-3}	-1.7986×10^{-5}	-3.1131×10^{-6}	3.3582×10^{-8}
$1.05 - 0.0001i$	2.5953×10^{-4}	-4.1480×10^{-3}	5.7072×10^{-3}	-1.9219×10^{-5}	-3.0912×10^{-6}	3.3578×10^{-8}
$1.05 - 0.001i$	3.0380×10^{-4}	-4.2042×10^{-3}	5.7340×10^{-3}	-3.0292×10^{-5}	-2.8851×10^{-6}	3.3365×10^{-8}
$1.06 - 0i$	4.4312×10^{-4}	-6.1325×10^{-3}	8.3223×10^{-3}	-2.3909×10^{-5}	-7.0740×10^{-6}	9.5221×10^{-8}
$1.06 - 0.0001$	4.5650×10^{-4}	-6.1500×10^{-3}	8.3291×10^{-3}	-2.6092×10^{-5}	-7.0178×10^{-6}	9.4923×10^{-8}
$1.06 - 0.001i$	5.7538×10^{-4}	-6.3079×10^{-3}	8.3928×10^{-3}	-4.5717×10^{-5}	-6.5021×10^{-6}	9.2010×10^{-8}
$1.07 - 0i$	1.3299×10^{-3}	-9.3811×10^{-3}	1.1714×10^{-2}	-5.5654×10^{-5}	-1.2716×10^{-5}	2.0198×10^{-7}
$1.07 - 0.0001i$	1.3546×10^{-3}	-9.4150×10^{-3}	1.1728×10^{-2}	-5.9216×10^{-5}	-1.2600×10^{-5}	2.0101×10^{-7}
$1.07 - 0.001$	1.5906×10^{-3}	-9.7383×10^{-3}	1.1852×10^{-2}	-9.1674×10^{-5}	-1.1531×10^{-5}	1.9177×10^{-7}

TABLE 2.1. Coefficients (dimensionless) for the approximation of the function $Q_b(x)$ for different values of m. See equation (2.2) in the text.

$$f(x) = \frac{1}{\sigma_x\sqrt{2\pi}} \exp\left[-\frac{(x-\bar{x})^2}{2\sigma_x^2}\right] , \tag{2.3}$$

where $\bar{x}$ and σ_x are the mean and standard deviation, respectively. Using equation (2.2) and expressing equation (2.3) as

$$f(x) = \sqrt{\frac{\omega}{\pi}} \exp(-\omega\bar{x}^2) \exp(-\omega x^2 - \gamma x) , \tag{2.4}$$

where $\omega = 1/(2\sigma_x^2)$ and $\gamma = -2\omega\bar{x}$, we can rewrite equation (2.1) as

$$b_h = \frac{\lambda^2 N}{4\pi n_w^2} \sqrt{\frac{\omega}{\pi}} \exp(-\omega\bar{x}^2) \sum_{j=0}^{k} \alpha_j \int_0^\infty x^{j+2} \exp(-\omega x^2 - \gamma x) dx . \tag{2.5}$$

Integration over x (Gradshteyn and Ryzhik, 1980, p. 337) leads to the result

$$b_h = \frac{\lambda^2 N}{8\pi n_w^2 \omega} \sqrt{\frac{1}{2\pi}} \exp\left(\frac{-\omega\bar{x}^2}{2}\right) \sum_{j=0}^{k} \alpha_j (2\omega)^{-j/2} (j+2)! \, \mathrm{U}_{-(j+3)}\left(\frac{\gamma}{\sqrt{2\omega}}\right) , \tag{2.6}$$

where $\mathrm{U}_\vartheta(y)$ is a parabolic cylinder function of order ϑ and argument y.

Since ϑ in equation (2.6) is a negative integer we can use the property

$$\mathrm{U}_{-n-1}(y) = \sqrt{\frac{\pi}{2}} 2^{n/2} \exp\left(\frac{y^2}{4}\right) \mathrm{i}^n\mathrm{erfc}\left(\frac{y}{\sqrt{2}}\right) \qquad n = 0, 1, 2, \ldots$$

to express the solution in terms of repeated integrals of the error function complement, defined as

$$\mathrm{i}^n\mathrm{erfc}(y) = \frac{2}{\sqrt{\pi}} \int_y^\infty \frac{(t-y)^n}{n!} \exp(-t^2)dt \; ; \qquad n = 1, 2, 3, 4, ...$$

$$\mathrm{i}^0\mathrm{erfc}(y) = \mathrm{erfc}(y) \; ; \qquad \mathrm{i}^{-1}\mathrm{erfc}(y) = \frac{2}{\sqrt{\pi}} \exp(-y^{\,2}) \, ,$$

also known as the complementary error function integral. The result is

$$b_h = \frac{\lambda^2 N}{8\pi\, n_w^2\, \omega} \sum_{j=0}^{k} \alpha_j \omega^{-j/2} (j+2)!\, \mathrm{i}^{j+2}\mathrm{erfc}\left(\frac{\gamma}{\sqrt{4\omega}}\right) . \tag{2.7}$$

Repeated application of the recurrence relationship

$$\mathrm{i}^n\mathrm{erfc}(y) = \frac{-y}{n}\mathrm{i}^{n-1}\mathrm{erfc}(y) + \frac{1}{2n}\mathrm{i}^{n-2}\mathrm{erfc}(y) \qquad n = 1, 2, 3, ...$$

permits us to express $\mathrm{i}^n\mathrm{erfc}(y)$ in terms of the error function complement ($\mathrm{erfc}(y) = 2/\sqrt{\pi}\int_y^\infty \exp(-t^2)\, dt$) and $\exp(-y^2)$, and hence allows equation (2.7) to be evaluated.

The effective efficiency factor for scattering, $\bar{Q}_b$, defined as the ratio of the total optical cross-section for scattering to the total geometrical cross-section (van de Hulst, 1957), is given by

$$\bar{Q}_b = \frac{\int_0^\infty Q_b(m,x)\, x^2 f(x) dx}{\int_0^\infty x^2 f(x) dx} \, . \tag{2.8}$$

Using the same approach as above, we can integrate equation (2.8) over x, with the result

$$\bar{Q}_b = \sum_{j=0}^{k} \alpha_j \omega^{-j/2} \frac{(j+2)!}{2!} \frac{\mathrm{i}^{j+2}\mathrm{erfc}(\gamma/\sqrt{4\omega})}{\mathrm{i}^2\mathrm{erfc}(\gamma/\sqrt{4\omega})} \, . \tag{2.9}$$

2.4 Gamma Distribution

We can choose $f(x)$ to be the gamma distribution

$$f(x) = \frac{\eta^{\nu}}{\Gamma(\nu)}\, x^{(\nu-1)} e^{-\eta x} \,, \tag{2.10}$$

where Γ is the gamma function, and ν and η are the parameters of the distribution. The two parameters are related to the mean $\bar{x}$, the mode x_m, and the standard deviation σ_x of the population:

$$\nu = \frac{\bar{x}}{\bar{x} - x_m} = \frac{\bar{x}^2}{\sigma_x^2} \tag{2.11a}$$

and

$$\eta = \frac{1}{\bar{x} - x_m} = \frac{\bar{x}}{\sigma_x^2} \,. \tag{2.11b}$$

Using equations (2.2) and (2.10), we can integrate equation (2.1) to find another analytical expression for the scattering coefficient:

$$b_h = \frac{\lambda^2\, N}{4\,\pi\, n_w^2} \sum_{j=0}^{k} \alpha_j \frac{(\nu)_{j+2}}{\eta^{j+2}} \,, \tag{2.12}$$

where $(\nu)_{j+2}$ is the particular case, $p = j + 2$, of the Pochhammer polynomial $(\nu)_p$, defined by the expression $(\nu)_p = \prod_{l=0}^{p-1}(\nu + l)$. For $k = 5$ and for a polydispersion with standard deviation $\sigma_x = 30\%\bar{x}$, the relative error in equation (2.12) is $< 3\%$ over the refractive index and size parameter range of interest.

We can also evaluate equation (2.8), obtaining another expression for the effective efficiency factor for scattering:

$$\bar{Q}_b = \sum_{j=0}^{k} \alpha_j \frac{(\nu+2)_j}{\eta^j} , \tag{2.13}$$

where the recursion property of the Pochhammer polynomial was used to set $(\nu)_{j+2}/(\nu)_j = (\nu+2)_j$.

2.5 Discussion

With the assumption that the scattering of light by heterotrophic bacteria obeys Mie theory and that marine bacteria can be characterized by a normal or gamma size distribution, I have derived simple expressions for the scattering coefficient of bacterial assemblages as a function of size, concentration, and refractive index.

The choice of whether to use a normal or gamma size distribution will depend on how well each distribution represents real data. Figure 2.2 shows the size distribution for bacterial assemblages from the Western North Atlantic. Data from different depths, stations, and geographical regions (Georges Bank, the Northeast Channel, and the Sargasso Sea) have been combined. A normal and a gamma distribution have been fitted to the data. Both distributions represent the data well, but some differences can be observed. However, when the standard deviation is $\leq$ 30% of the mean, the difference between estimates of b_h using a normal or a gamma distribution is $\leq$ 6% (Fig. 2.3). For such cases, the use of the solution for the gamma distribution (equation (2.12)) has the advantage of being easier to compute.

Approximations for different optical properties of water clouds have been given recently by Chýlek *et al.* (1992*a, b*) and Damiano (1992). Their results are also based on polynomial approximations for the optical efficiency factors. They use, however, a dimensional size variable (the radius) to build their approximations. One

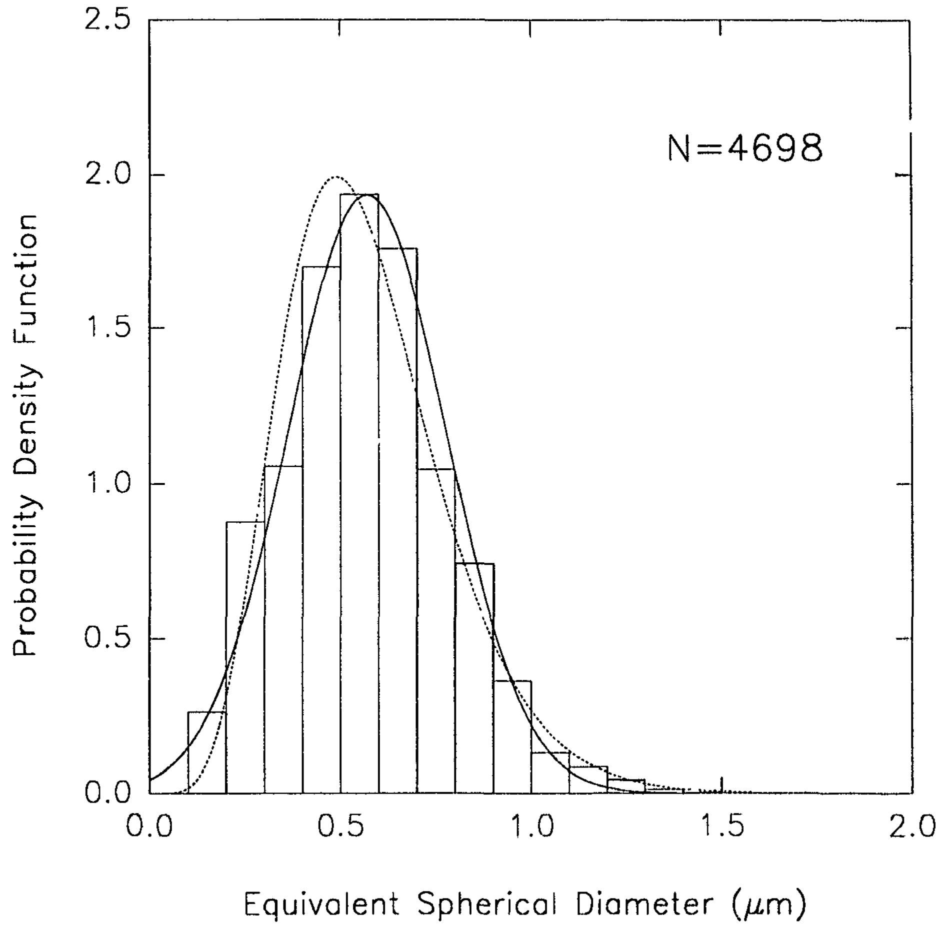

FIGURE 2.2. Bacterial size distribution for the Western North Atlantic. Combined data from Georges Bank, the Northeast Channel (Gulf of Maine), and the Sargasso Sea. A normal (solid line) and a gamma (dashed line) distribution have been fitted to the data.

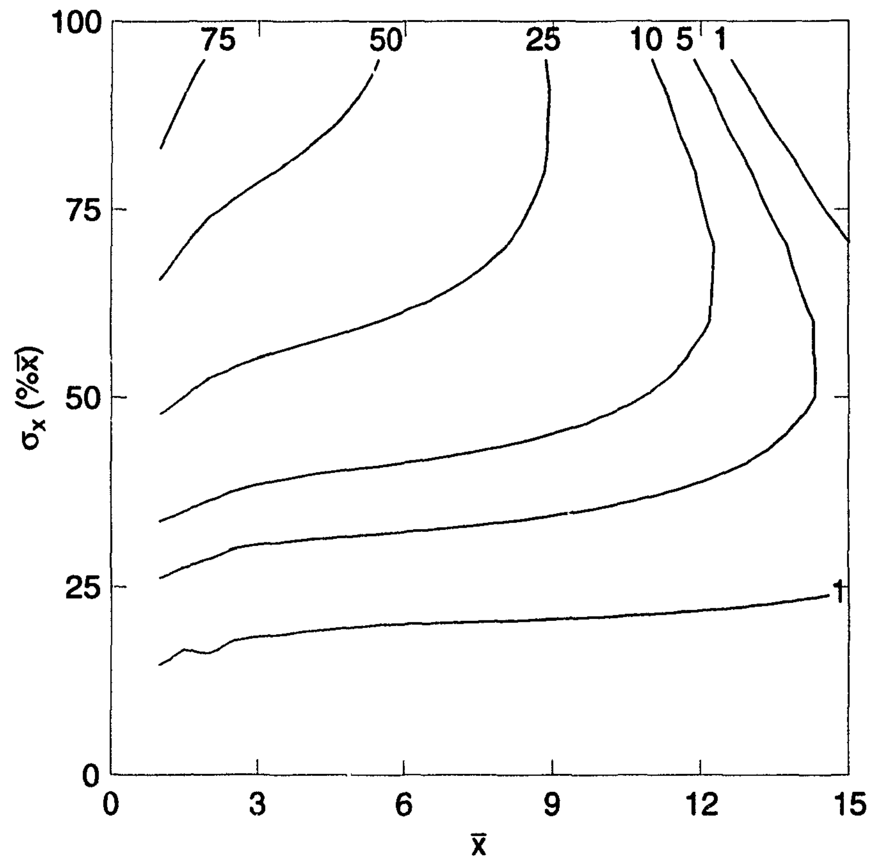

FIGURE 2.3. Relative difference (%) between b_h computed using a normal and a gamma distribution for $f(x)$ in equation 2.1.

difference from the approach followed here (based on the dimensionless x) is that, for a given refractive index, their approximations require a different set of empirical coefficients at each wavelength. On the contrary, when the size variable is expressed in a dimensionless form (equation 2.2) the empirical coefficients are wavelength independent if the refractive index does not vary significantly with wavelength, which is the case for heterotrophic bacteria (Morel and Ahn, 1990; Stramski and Kiefer, 1990). When Chýlek *et al.*, 1992*a, b* and Damiano (1992) use a gamma-type size distribution for the water droplets, they obtain a result similar to equation (2.12) and to that given in Ulloa *et al.* (1992); they do not give solutions for the case of a normal size distribution.

The results presented here can be applied to a variety of problems such as modelling light penetration in the ocean (*e.g.*, Morel, 1988; Sathyendranath and Platt, 1988), interpretation and modelling of ocean color for remote sensing (*e.g.*, Gordon and Morel, 1983; Gordon *et al.*, 1988), and the assessment of primary production by remote sensing (Platt and Sathyendranath, 1988) or by measurements of *in situ* optical properties such as the attenuation coefficient (Siegel *et al.*, 1989). In none of these subjects, so far, has the independent role of heterotrophic bacteria been taken into account.

CHAPTER 3

Bacterial Scattering in Waters of the Western North Atlantic

3.1 Introduction

Early measurements of the absorption properties of a marine heterotrophic bacterium in culture were reported by Yentsch (1962). More recently, measurements of both the absorption and scattering properties of heterotrophic bacteria have been made on cultures isolated from marine environments (Kopelevich *et al.*, 1987; Morel and Ahn, 1990; Stramski and Kiefer, 1990). These latter results show that heterotrophic bacteria are much more efficient as scatterers of light than as absorbers and suggest that in natural waters bacteria could contribute significantly to the scattering of light. However, no direct measurements of the contribution of heterotrophic marine bacteria to the absorption and scattering of light in the ocean have yet been made, although it has been recognized that bacteria can affect significantly *in situ* measurements of optical properties such as the attenuation coefficient (Spinrad *et al.*, 1989*a, b*). Lacking yet a direct approach of estimating bacterial scattering in natural waters, an alternative approach is to combine the physical theory of light scattering with data on bacterial size and abundance.

The size distribution of bacteria in nature can differ significantly from that of laboratory cultures (Güde, 1989; Robertson and Button, 1989), since the latter represent a selected group, free of predators. On the other hand, information on bacterial size in the ocean is still limited. Although bacterial size can be measured in cultures using electronic particle sizers (Kogure and Koike, 1987), bacterial sizes in natural samples are still most commonly determined using epifluorescence microscopy (*e.g.*, Cho and Azam, 1990), a tedious and time-consuming method. With most particle sizers it is not possible to distinguish between living and non-living particles, and in most cases the resolution of the instruments has been insufficient to yield reliable information on particles smaller than 1 μm and therefore on the size ranges comprising heterotrophic bacteria (Kogure and Koike, 1987). This work is based on detailed size measurements of bacterial natural samples, obtained with image-analyzed, epifluorescence microscopy.

The primary objective of this chapter is to use measurements of abundance and size distribution of marine bacteria to estimate the importance of heterotrophic bacteria as light scatterers at sea. The general approach is to apply the exact Mie theory (as described in Chapter 1) to field data on bacterial size and abundance. Since we made no direct measurements of refractive index during our cruises, I use the refractive indices that have been previously reported (Morel and Ahn, 1990; Stramski and Kiefer, 1990). For the scattering coefficient, I compare these results with those obtained using the analytical expression derived in Chapter 2. I then examine the potential contribution of bacteria to the scattering properties of seawater. Finally, I examine recent data (Li *et al.*, 1992) on the relationship between bacterial abundance and pigment concentration and evaluate the utility of pigment data as a basis for predicting the magnitude of scattering by bacteria.

3.2 Material and Methods

3.2.1 Sampling and Size Measurements. Samples for bacterial counts and size measurements were taken from C.S.S. *Hudson* during August–September, 1988. Data from two stations on Georges Bank, two stations in the Northeast Channel (Gulf of Maine), and one station in the Sargasso Sea are presented. They represent waters that varied over almost 2 orders of magnitude in their pigment concentration (see Fig. 3.2). Water samples were collected with 30-L Niskin bottles from different depths and were fixed with prefiltered formaldehyde (0.2-μm pore size Nucleopore filters) to a final concentration of 2%, and stored at 4°C in the dark until further analysis. Pigment data and additional information are given by Irwin *et al.* (1990*a*,*b*).

In the laboratory, cells were stained with 4′,6-Diamidino-2-phenylindole dihydrochloride hydrate, DAPI, according to Porter and Feig (1980) and filtered onto 0.2-μm pore size black Nucleopore filters using a vacuum at a pressure of $<1.3\times10^4$ Pa. The counting was performed with a Leitz Orthoplan epifluorescence microscope under 1000×. Three slides per depth, with five to seven fields per slide, were counted using an ocular grid reticule. For the size determination, pictures (Kodak Ektachrome, P800/1600, slides) of randomly selected fields were taken. The slides were projected to a final magnification of 1500×. The images of the slide projection were captured with a video camera, and then digitized and processed with an Image Analyzer. A Newvicon tube camera and an Oculus-300 (Coreco Inc.) framegrabber video digitizer board were used in our case; otherwise, the configuration of the system was the same as the one described by Campana (1987). The reported sizes correspond to the equivalent spherical diameter D derived from the measured projected areas.

3.2.2 Optical Characteristics and Contribution of Bacteria to Total Scattering and Backscattering. The dimensionless effective efficiency factors for scattering and backscattering, $\bar{Q}_c$ and $\bar{Q}_{b_b}$ respectively, the scattering and backscatering coeficients, b_h and b_{bh} with dimensions of [L^{-1}], and the dimensionless backscattering ratio $\tilde{b}_b$ were obtained by numerical computations applying the Mie equations to the measured size distribution and using a refractive index $m = 1.05 - 0.0001i$ (Morel and Ahn, 1990; Stramski and Kiefer, 1990; see also Chapter 1). The scattering coefficient b_h was also computed using the expression derived in Chapter 2:

$$b_h = \frac{\lambda^2 N}{4\pi n_w^2} \sum_{j=0}^{k} \alpha_j \frac{(\nu)_{j+2}}{\eta^{j+2}} , \tag{3.1}$$

where λ is the wavelength of light in vacuum, N is the number of bacteria per unit volume, n_w is the refractive index of the medium, water ($n_w = 1.34$), α_j are empirical coefficients given in Table 2.1 (Chapter 2), and ν and η are the parameters of the gamma distribution, which in turn are related to mean and the standard deviation of the bacterial population (see equation (2.11) a,b).

The total scattering coefficient (in m^{-1}) at 550 nm was obtained from the empirical relationship (Gordon and Morel, 1983)

$$b[550] = 0.30C^{0.62} \;, \tag{3.2}$$

where C is the phytoplankton pigment concentration (chlorophyll a +phaeopigments) in milligrams per cubic meter. The total backscattering coefficient was calculated according to Morel (1988):

$$b_b[550] = 0.30C^{0.62}(2 \times 10^{-3} + 5 \times 10^{-3}(2 - \log C)) + b_{bw} \;, \tag{3.3}$$

where b_{bw} is the molecular backscattering coefficient due to pure seawater at 550 nm, and equal to half of its molecular scattering coefficient, b_w. The value of $b_w = 0.0019$ m^{-1} was obtained from Morel (1974). In equation (3.3), the particle backscattering coefficient b_b' (first term on the right side of the equation) is modelled as the product of the particle scattering coefficient b' (obtained from equation (3.2)) and the particle backscattering ratio $\tilde{b}_b'$ ($b_b' = b'\,\tilde{b}_b'$). The latter is assumed to be a function of the phytoplankton pigment concentration C: the sum of a constant term, equal to 0.2%, and a term decreasing proportionally to $\log_{10} C$, from 2%, when $C = 10^{-2}$ mg m^{-3}, to zero, when $C = 10^2$ mg m^{-3}.

3.3 Results

A total of 32 bacterial size-spectra was examined (Table 3.1). The observed mean equivalent spherical diameter D varied from 0.50 to 0.65 μm among samples. These values are within the range of those observed for natural samples from the Southern California Bight and waters off the Scripps Institution of Oceanography Pier (Fuhrman, 1981), as well as those from waters associated with a warm-core Gulf Stream ring (Ducklow, 1986). They are slightly higher than those reported by Cho and Azam (1990) for the central North Pacific gyre and coastal waters off California, and by Fuhrman *et al.* (1989) for the Sargasso Sea. Compared with marine bacteria in culture, they are within the range reported by Stramski and Kiefer (1990), but they are lower than those reported by Robertson and Button (1989) and in the lower end of the range reported by Morel and Ahn (1990).

A selected example of size distribution at each sampling location is shown in Figure 3.1. The observed distributions agree well with those previously published (Fuhrman, 1981; Robertson and Button, 1989), and are believed to be representative of natural assemblages. Gamma distributions fitted to the data are also shown. Figure 3.2 shows a plot of length of the major axis versus length of the minor axis for all the data (N = 4698). The ratio of these two variables is a measure of the shape. For a sphere this ratio is 1. The frequency distribution and the cumulative frequency for the ratio of major axis to minor axis show that most bacteria ($>$ 95%) have a length-to-width ratio of $\leq$ 2, and that more than half of them have a ratio of $\leq$ 1.25. These results give an estimate of how closely the shape of bacteria in nature approaches a sphere.

The optical characteristics of bacteria for two wavelengths, λ = 440 and 550 nm, are given in Table 3.2. Values of b_h obtained from the derived analytical expression, equation (3.1), agree well with those obtained from the complete Mie computations. I preferred to report the results for the comparison when the observed mean and

Station	Depth	Bacterial No.	D	SD	N
GB1	0	2.73	0.55	0.19	246
23 Aug.	5	2.07	0.52	0.18	181
	10	2.42	0.54	0.18	176
	15	2.01	0.50	0.18	204
	25	2.07	0.62	0.23	201
	35	2.32	0.50	0.18	174
GB2	0	2.06	0.60	0.20	207
24 Aug.	5	2.29	0.53	0.18	157
	10	1.53	0.57	0.21	158
	15	1.70	0.52	0.19	204
	28	2.26	0.55	0.19	206
	40	1.91	0.60	0.22	246
NC1	0	2.07	0.63	0.22	217
27 Aug.	10	2.20	0.55	0.21	155
	20	2.95	0.62	0.22	236
	45	1.83	0.56	0.19	221
	70	0.51	0.59	0.19	132
	90	0.50	0.62	0.17	96
NC2	0	2.90	0.55	0.20	235
28 Aug.	10	3.23	0.58	0.20	222
	25	2.39	0.62	0.25	174
	50	0.46	0.60	0.22	74
	75	0.34	0.63	0.23	54
	100	0.22	0.61	0.20	69
SS1	0	0.42	0.53	0.19	40
16 Sep.	25	0.40	0.52	0.14	76
	50	0.45	0.57	0.22	77
	72	0.49	0.56	0.24	61
	125	0.20	0.52	0.19	67
	150	0.13	0.65	0.22	40
	175	0.12	0.62	0.20	26
	200	0.14	0.63	0.24	66

TABLE 3.1. Bacterial concentration and size in Georges Bank (GB; 41°43′N, 67°29′W), Northeast Channel (NC; 42°20′N, 66°48′W), and Sargasso Sea (SS; 36°02′N, 65°09′W) during summer 1988. The concentration is expressed in units of 10^{12} cells m^{-3} and the depth in meters. D is the mean equivalent spherical diameter in micrometers over N observations, and SD is the standard deviation of the mean.

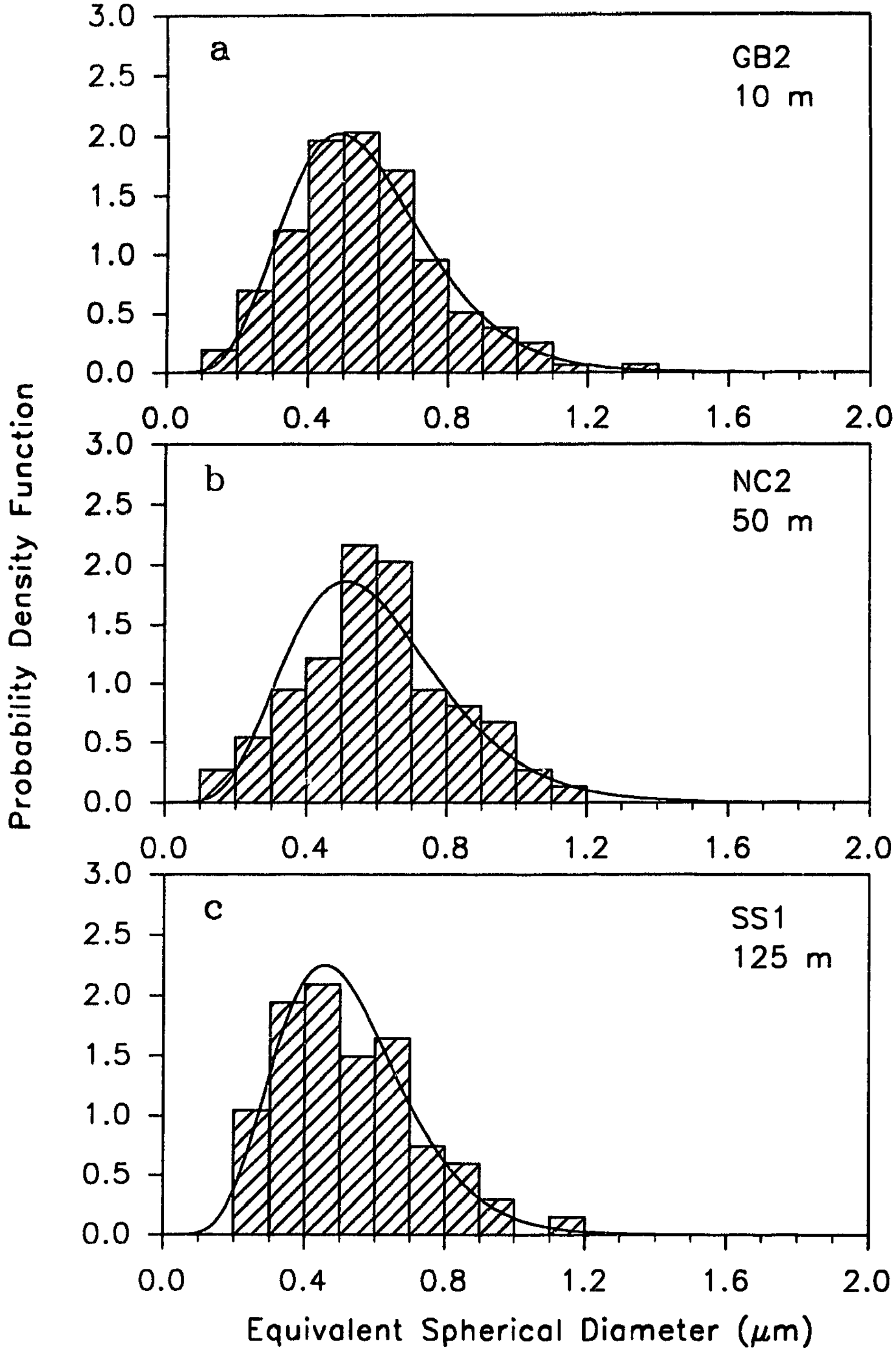

FIGURE 3.1. Bacterial size distribution (probability density function) of a selected sample in (*a*) Georges Bank, (*b*) Northeast Channel, and (*c*) Sargasso Sea. The solid lines correspond to gamma distributions fitted to the data.

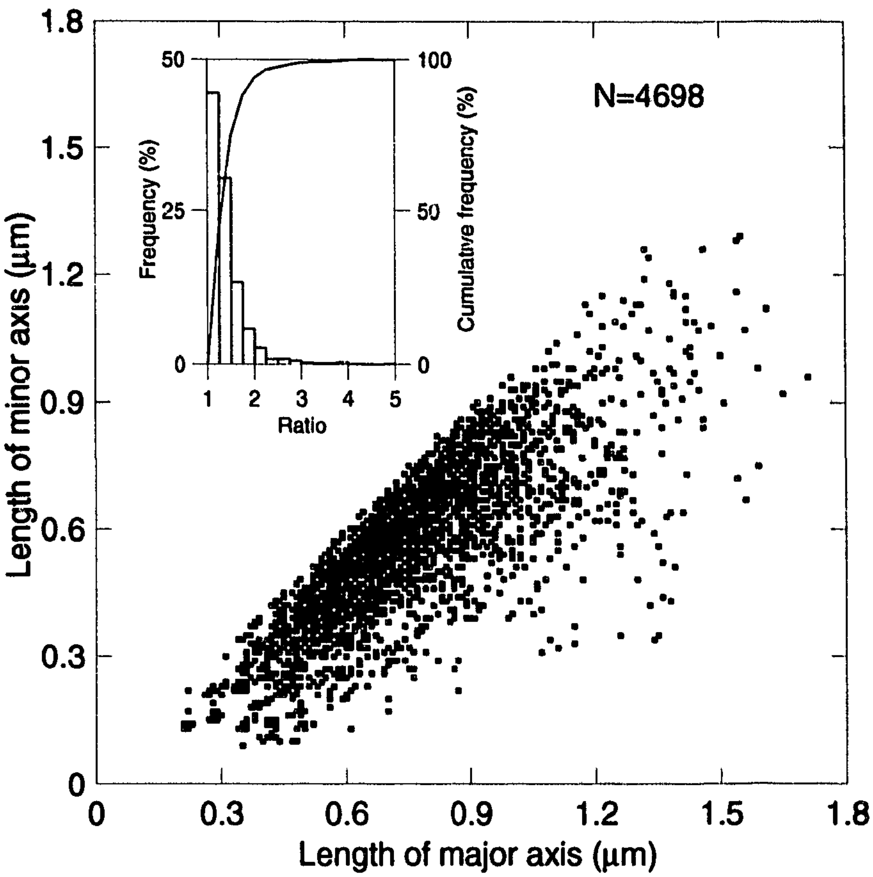

FIGURE 3.2. Plot of length of the minor axis versus length of the major axis. The frequency distribution and the cumulative frequency for the ratio (major/minor) are given in the inset. This ratio is 1 for a sphere.

standard deviations of the size (Table 3.1) at each sampling depth are used to derive ν and η, rather than using ν and η fitted directly to the data. The rationale for this choice was that in practice, size data are usually available in the literature as mean and standard deviation.

Figures 3.3 and 3.4 show comparisons between the scattering and backscattering coefficients due to bacteria (b_h and b_{bh}) and the total scattering and backscattering coefficients (b and b_b), respectively, as derived from the pigment data. The values of b_h and b_{bh} at each depth are from Table 3.2.

3.4 Discussion and Conclusions

From the results presented here, the contribution of bacteria to the total scattering b would be on average around 10% in Georges Bank (range 7–17%) and the Sargasso Sea (range 3–16%), and 30% in the Northeast Channel (range 9–57%). With respect to the total backscattering coefficient, the bacterial contribution would be on average around 7% in Georges Bank (range 5–9%), 12% in the Northeast Channel (range 3–22%), and 3% in the Sargasso Sea (range 1–4%). The apparent higher contribution to b and b_b by bacteria in the Northeast Channel, as compared with the other locations, can be explained by the observed high bacterial abundance in the low-chlorophyll, summer-stratified, surface waters. In Georges Bank, the total scattering coefficient, and therefore the total backscattering coefficient, are probably underestimated, since resuspended sediments are expected to be present in the water column. Their contribution is not taken into account by equations (3.2) and (3.3), which were derived for case 1 waters, i.e., waters where phytoplankton and their derivative products are believed to be the predominant components influencing the optical properties of the water body (Morel and Prieur, 1977; Gordon and Morel, 1983; Morel, 1988).

Kopelevich *et al.* (1987) postulated that the relative contribution of bacteria to the scattering of light would be directly related to their absolute concentration

Station	Depth	$\lambda = 440$ nm						$\lambda = 550$ nm					
		$\bar{Q}_b$	$\bar{Q}_{b_b}$	b_h	b_h^*	b_{bh}	$\tilde{b}_b$	$\bar{Q}_b$	$\bar{Q}_{b_b}$	b_h	b_h^*	b_{bh}	$\tilde{b}_b$
GB1	0	0.208	0.961	0.151	0.162	0.697	0.0046	0.131	0.923	0.095	0.103	0.669	0.0071
	5	0.201	0.951	0.098	0.098	0.466	0.0047	0.127	0.925	0.062	0.062	0.453	0.0073
	10	0.211	0.947	0.133	0.129	0.597	0.0045	0.133	0.927	0.084	0.081	0.584	0.0070
	15	0.180	0.960	0.080	0.085	0.426	0.0053	0.113	0.914	0.050	0.054	0.405	0.0081
	25	0.282	0.973	0.202	0.216	0.696	0.0034	0.180	0.933	0.129	0.138	0.667	0.0052
	35	0.182	0.942	0.092	0.099	0.478	0.0052	0.114	0.914	0.058	0.062	0.469	0.0080
GB2	0	0.261	0.967	0.173	0.167	0.641	0.0037	0.166	0.937	0.110	0.106	0.621	0.0056
	5	0.199	0.950	0.113	0.115	0.538	0.0048	0.125	0.909	0.071	0.073	0.515	0.0073
	10	0.252	0.967	0.111	0.113	0.424	0.0038	0.161	0.942	0.070	0.072	0.413	0.0059
	15	0.201	0.966	0.075	0.086	0.361	0.0048	0.126	0.931	0.053	0.055	0.387	0.0074
	28	0.221	0.990	0.133	0.134	0.597	0.0045	0.140	0.940	0.084	0.085	0.567	0.0067
	40	0.277	0.983	0.171	0.172	0.607	0.0036	0.176	0.936	0.109	0.110	0.578	0.0053
NC1	0	0.288	0.987	0.205	0.214	0.704	0.0034	0.183	0.947	0.131	0.137	0.676	0.0052
	10	0.234	0.984	0.141	0.148	0.591	0.0042	0.148	0.930	0.089	0.094	0.558	0.0063
	20	0.286	0.972	0.288	0.292	0.976	0.0034	0.182	0.949	0.183	0.186	0.953	0.0052
	45	0.215	0.961	0.108	0.115	0.483	0.0045	0.136	0.924	0.068	0.073	0.464	0.0068
	70	0.243	0.969	0.038	0.037	0.153	0.0040	0.154	0.935	0.024	0.024	0.148	0.0061
	90	0.225	0.989	0.036	0.039	0.156	0.0044	0.142	0.903	0.022	0.025	0.143	0.0063
NC2	0	0.228	0.976	0.177	0.183	0.760	0.0043	0.144	0.916	0.112	0.116	0.714	0.0064
	10	0.243	0.960	0.230	0.237	0.909	0.0039	0.154	0.957	0.146	0.151	0.906	0.0062
	25	0.322	0.986	0.270	0.278	0.826	0.0031	0.207	0.942	0.173	0.178	0.790	0.0046
	50	0.264	0.938	0.039	0.042	0.146	0.0037	0.168	0.926	0.025	0.026	0.138	0.0055
	75	0.304	0.979	0.036	0.037	0.117	0.0032	0.194	0.935	0.023	0.024	0.111	0.0048
	100	0.254	0.966	0.018	0.019	0.070	0.0038	0.161	0.959	0.012	0.012	0.069	0.0059
SS1	0	0.199	0.946	0.020	0.022	0.097	0.0047	0.126	0.924	0.013	0.014	0.095	0.0074
	25	0.167	0.954	0.015	0.015	0.086	0.0057	0.105	0.913	0.009	0.009	0.082	0.0087
	50	0.277	0.994	0.036	0.035	0.128	0.0036	0.177	0.945	0.023	0.023	0.122	0.0053
	72	0.285	0.990	0.040	0.042	0.138	0.0035	0.182	0.948	0.025	0.027	0.132	0.0052
	125	0.221	0.972	0.011	0.010	0.049	0.0044	0.140	0.912	0.007	0.006	0.046	0.0065
	150	0.308	0.977	0.015	0.015	0.046	0.0032	0.197	0.947	0.009	0.009	0.045	0.0048
	175	0.265	0.940	0.010	0.011	0.037	0.0035	0.169	0.948	0.007	0.007	0.037	0.0056
	200	0.311	1.002	0.016	0.016	0.051	0.0032	0.199	0.948	0.010	0.010	0.048	0.0048

TABLE 3.2. Optical characteristics of heterotrophic bacteria in Georges Bank, Northeast Channel, and Sargasso Sea at 440 and 550 nm obtained through Mie computations applied to the observed size distributions, and using a refractive index of $1.05 - 0.0001i$. The scattering coefficients obtained from the derived analytical expression (b_h^*) are also given. The depth is in meters, b_h and b_h^* in reciprocal meters, and b_{bh} in units of $10^{-3}\,\mathrm{m}^{-1}$.

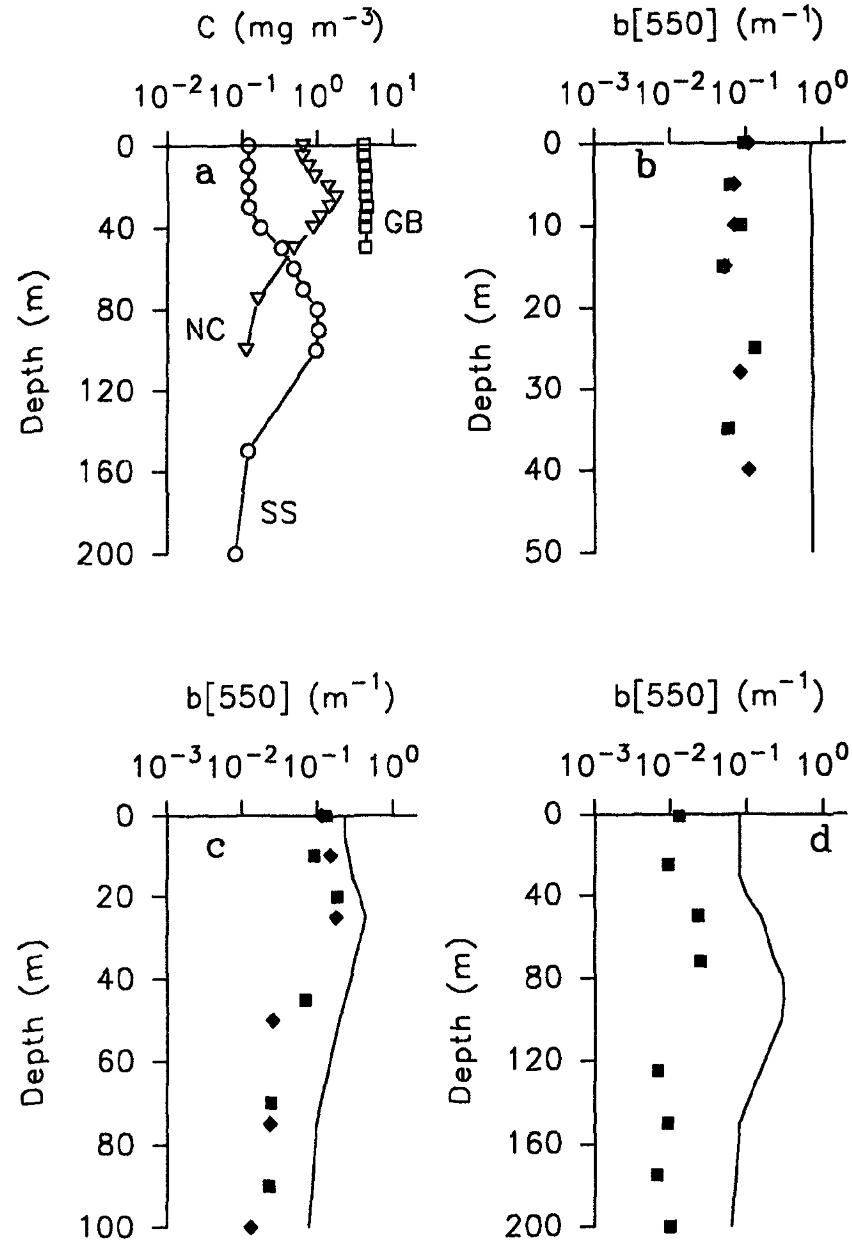

FIGURE 3.3. (*a*) Average vertical profiles of phytoplankton pigment concentration C (chlorophyll a + phaeopigments) in Georges Bank (GB), Northeast Channel (NC), and Sargasso Sea (SS), and comparison between the scattering coefficient at 550 nm due to pure sea water (dotted line), heterotrophic bacteria (symbols; squares represent station 1 and diamonds station 2), and the total scattering coefficient at the same wavelength (solid line) derived from the pigment data in (*b*) Georges Bank, (*c*) Northeast Channel, and (*d*) Sargasso Sea.

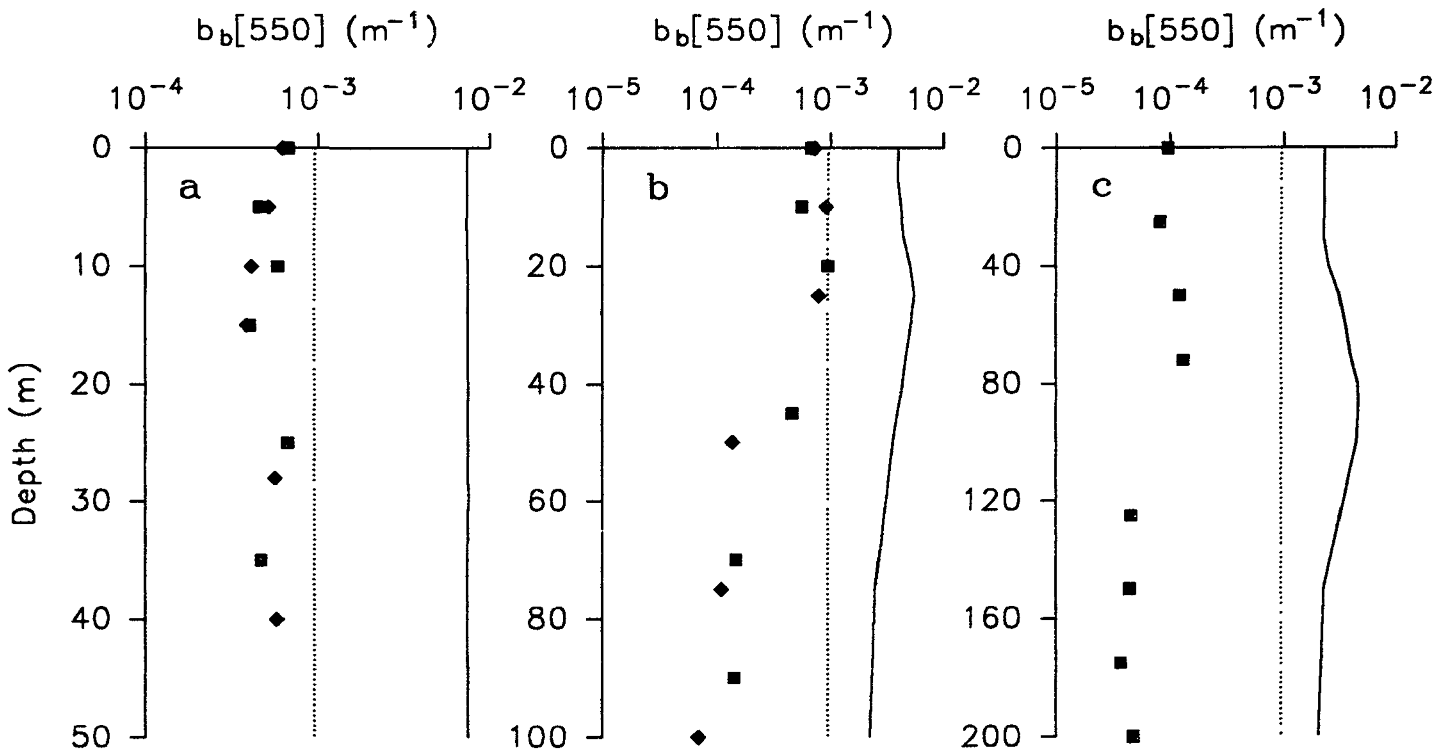

FIGURE 3.4. Vertical profiles of the backscattering coefficients at 550 nm in (*a*) Georges Bank, (*b*) Northeast Channel, and (*c*) Sargasso Sea, derived from the pigment data in Figure 3.3. Symbols and line types as in Figure 3.3 but for backscattering.

and that in oligotrophic waters their contribution would be negligible. Stramski and Kiefer (1990), on the contrary, suggested that the contribution of bacteria would be more significant in oligotrophic waters, owing to their larger total cross section, as compared with phytoplankton. Morel and Ahn (1990), on the other hand, argued that their contribution would be independent of the trophic state, providing that there is a correlation between bacterial numbers and phytoplankton pigment concentration.

The results presented in this chapter show that bacteria could contribute significantly to the total scattering coefficient in any of the three different environments studied. However, their contribution would depend not so much on the trophic status of the ecosystem as on the local relative abundance (and optical properties) of each of the major components influencing the optical properties of the sea water. The stations that showed the highest contribution from bacteria to the total scattering were those in the Northeast Channel, which represent an intermediate case between the phytoplankton-rich waters of Georges Bank and the oligotrophic waters of Sargasso Sea.

With respect to backscattering, the bacterial contribution to the total backscattering coefficient seems to be somewhat lower than for the total scattering coefficient, but nevertheless significant. However, contrary to the case for equation (3.2), no empirical evidence has yet been given in support of equation (3.3), and therefore results from the comparison between bacterial backscattering and total backscattering are less certain. Moreover, theoretical and laboratory results (Morel and Bricaud, 1981*b*; Bricaud *et al.*, 1983) show that phytoplankton have a very low backscattering ratio ($\tilde{b}_b < 0.1\%$), even lower than bacteria (see Table 3.2), which would weaken any relationship between total backscattering and pigment concentration. Notice, however, that in some cases (for example surface waters of the Northeast Channel) the backscattering due to bacteria is commensurate with that due to pure sea water, which in turn has been shown to make a significant contribution to the total backscattering coefficient (Morel and Prieur, 1977).

Several authors (Linley *et al.*, 1983; Bird and Kalff, 1984; Cole *et al.*, 1988; Cho and Azam, 1990) have found a significant positive relationship between bacterial abundance and phytoplankton chlorophyll concentration in the euphotic zone of different aquatic ecosystems. These results have been combined with equations (3.2) and (3.3) to predict the bacterial scattering and backscattering coefficients from pigment concentration (Morel and Ahn, 1990; 1991).

However, new results, including some from the same cruise that yielded the bacterial data presented here (Li *et al.*, 1992), show a high degree of scatter in the relation between bacteria and pigments within regions. For Georges Bank a regression of bacterial abundance on chlorophyll concentration gave an r^2 of 0.362 (N = 100), while for the Sargasso Sea the same procedure gave an r^2 of 0.194 (N = 62). When data from different cruises were combined (N = 364), only 29% of the variance in bacterial abundance could be explained by pigments (Fig. 3.5). Other authors (*e.g.*, Ducklow, 1986; McManus and Peterson, 1988; Karl *et al.*, 1991) have also found correlations between bacterial abundance and pigment concentration to be weak. If bacteria contribute significantly to the total scattering, as the present evidence suggests, their lack of, or low correlation with, pigments would account for some of the variability observed for the relationship between total scattering and pigments (Gordon and Morel, 1983; their Fig. 5*a*).

By examining new data on bacterial abundance versus pigment concentration, I conclude that although a positive relationship may exist sometimes between bacterial abundance and pigment concentration when comparisons are made across ecosystems (Bird and Kalff, 1984), this is not always the case. Moreover, looking at the relationship within ecosystems, it seems difficult to predict bacterial numbers from pigment data, and thus to derive the optical properties of bacteria relying on

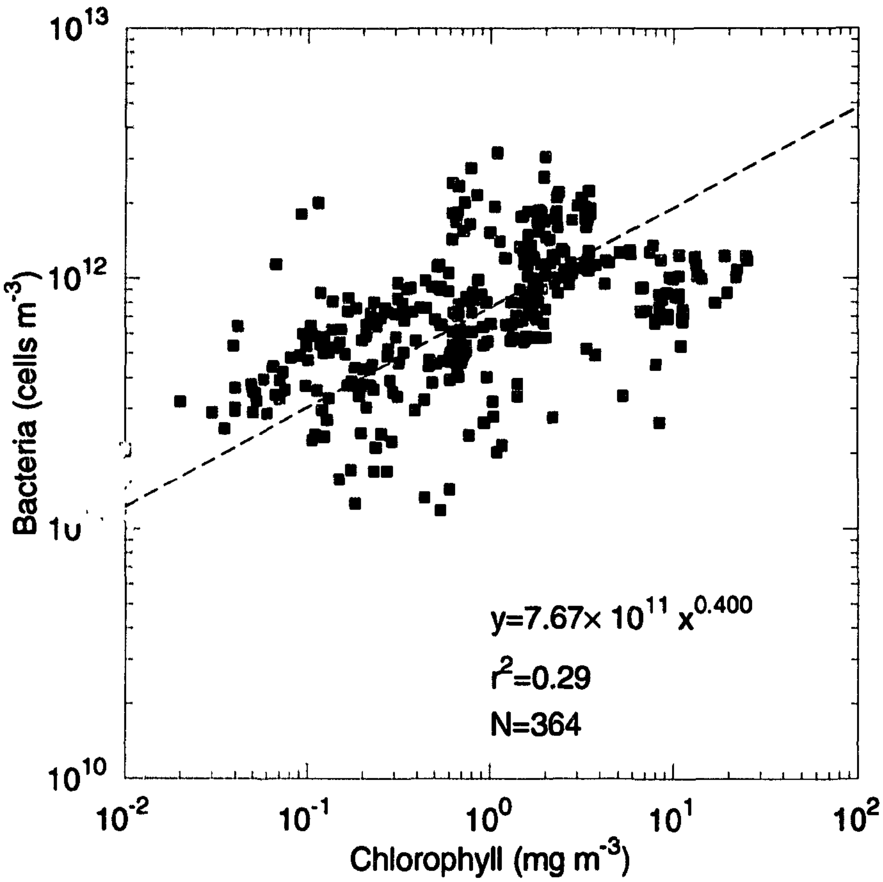

FIGURE 3.5. Bacterial abundance versus chlorophyll concentration from different cruises in the Western North Atlantic. The straight dashed line corresponds to the geometric mean model II regression. Data from Li *et al.* (1992).

pigment data. This conclusion emphasizes the utility of using field data on bacterial abundance, as has been done here, to calculate their contribution to scattering.

CHAPTER 4

Effect of Sub-micrometer Particles on the Particle Backscattering Ratio

4.1 Introduction

For many problems in optical oceanography the interest is on the portion of the light that is scattered in the backward direction, with respect to the incident light, rather than on the total scattered light. For example, the spectral irradiance reflectance (or ocean colour) is related to the ratio of the total backscattering and the total absorption coefficients, b_b/a (Gordon *et al.* 1975; Morel and Prieur, 1977). Measurements of the volume scattering function in the ocean (*e.g.*, Petzold, 1972) show that most of the scattering is in the forward direction, a consequence of the presence of particles in suspension (even in the most clear oceanic waters), and that the ratio of backscattering to total scattering is very small.

Recent studies (Morel and Ahn, 1991; Stramski and Kiefer, 1991) indicate that microorganisms, particularly phytoplankton and heterotrophic bacteria, could account for most of the total scattering in the ocean, but only for a small fraction of the backscattering; most of the backscattering would be due to the presence of high concentrations of sub-micrometer, detrital particles of organic origin. Early models of light scattering by marine particles (Gordon and Brown, 1972; Brown and Gordon, 1973, 1974; Morel, 1973) had already suggested that most of the backscattering could be due to high concentrations of sub-micrometer, organic particles. However, the existence of these particles in large numbers has only been demonstrated recently (Koike *et al.*, 1990; Longhurst *et al.*, 1992). Their optical properties have not been measured so far, and their occurrence in high concentrations in most of the world's oceans remains to be confirmed. Due to their small size and high backscattering efficiency, these particles would be major contributors to the backscattering coefficient, but not to the total scattering or absorption coefficients.

In current bio-optical models, the backscattering coefficient due to particles, b'_b, is commonly modelled as the product of the backscattering ratio, $\tilde{b}'_b = b'_b/b'$, and the scattering coefficient, b' (*e.g.*, Sathyendranath and Platt, 1988; Gordon *et al.*, 1988; Morel, 1988):

$$b'_b = \tilde{b}'_b \, b' \; . \tag{4.1}$$

The particle total scattering coefficient b' is usually nonlinearly related to the phytoplankton pigment concentration (see equation (3.2) in Chapter 3), based on the empirical results given by Gordon and Morel (1983). The particle backscattering ratio $\tilde{b}'_b$, on the other hand, is assumed to be constant (*e.g.*, Sathyendranath and Platt, 1988) or to covary inversely with pigment concentration (Gordon *et al.*, 1988; Morel, 1988); with any of these two assumptions, the backscattering coefficient becomes a function of the pigment concentration. Since phytoplankton is considered to contribute significantly to the total scattering coefficient, a relationship between b' and pigments is predictable. However, it is not evident that the backscattering ratio, and hence the backscattering coefficient, should covary with pigments, particularly if sub-micrometer particles are responsible for most of the backscattering, and not phytoplankton.

The optical properties of marine particles have been studied extensively using Mie theory (*e.g.*, Gordon and Brown, 1972; Morel, 1973; Kishino, 1980; Bricaud and Morel, 1986; Kitchen and Zaneveld, 1990; Stramski and Kiefer, 1991; Ulloa *et al.*, 1992). The backscattering ratio, however, to my knowledge, has only been studied for the case of monodispersions or polydispersions with normal or log-normal size distributions (Morel and Bricaud, 1981*b*, 1986), *i.e.*, for the case of a particular class of particles (*e.g.*, phytoplankton or bacteria) rather than for the total particle suspension.

In this chapter, I use Mie theory to examine how changes in the particle size distribution of the total particle suspension (represented by a Junge-type distribution) affect the backscattering ratio. I show that the backscattering ratio is largely controlled by sub-micrometer particles and that its magnitude varies directly and strongly with the absolute value of the exponent in the Junge-type distribution (the slope in a log-log plot). An inverse relationship between the backscattering ratio and the chlorophyll concentration is predicted, based on empirical relationships between the exponent of the Junge-type distribution of particles and the chlorophyll concentration.

4.2 The Backscattering ratio for Polydispersions with a Junge-type Distribution

The backscattering ratio $\tilde{b}_b'$ for a polydispersion of particles with refractive index m is given by (see equations (1.4) and (1.14) in Chapter 1)

$$\tilde{b}_b' = \frac{\int_{x_{\min}}^{x_{\max}} Q_{b_b}(m,x)x^2 f(x)dx}{\int_{x_{\min}}^{x_{\max}} Q_b(m,x)x^2 f(x)dx} \,, \tag{4.2}$$

where Q_b and Q_{b_b} are the efficiency factors for scattering and backscattering, respectively; $x = \pi D n_w/\lambda$ is the size parameter, where D is the diameter of the particles, n_w is the refractive index of of the medium (*i.e.*, sea water) and λ is the wavelength of light in vacuum; and $f(x)$ is the probability density function, such that the size distribution is $F(x) = Nf(x)$, where N is the total number of particles per unit volume. The efficiency factors Q_b and Q_{b_b} can be computed using Mie theory (see Chapter 1), assuming that the particles are spherical and optically homogeneous. Note that $\tilde{b}_b'$ does not depend on the absolute number of particles present in the water or in each size class, but only on the shape of the size distribution or the relative abundance between size classes. In this chapter, the absolute particle size D (the diameter in micrometers) is considered rather than the dimensionless size parameter x, since, as it will be shown, the backscattering ratio is wavelength-independent for particles that obey a Junge-type distribution.

The size distribution of the total particle suspension (living and non-living material) and of the pelagic organisms (living material) in aquatic ecosystems has been shown to be well represented by a Junge-type distribution (Bader, 1970; Sheldon *et al.*, 1972; Platt *et al.*, 1984; Rodriguez and Mullin, 1986), for which the probability density function $f(D)$ is

$$f(D) = K\, D^{-\xi}\ , \tag{4.3}$$

where $K = (\xi - 1)/(D_{\min}^{1-\xi} - D_{\max}^{1-\xi})$, $D_{\min}$ and $D_{\max}$ are the lower and upper limits of the size range under consideration, and ξ is an empirically-determined coefficient ~ 4. For the size distribution of aquatic organisms, the size variable commonly considered is weight (or biovolume) and not the number of particles and their diameter; in such cases the exponent in the normalized biomass size spectra becomes $(3-\xi)$, *i.e.*, ~ -1 (Platt and Denman, 1977). This latter exponent has been derived theoretically, based on energetic principles (Platt and Denman, 1977, 1978). For total particle size spectra, the observed range for ξ varies from 3 to 5 (Jonasz, 1983), while for living particles, it is restricted to the range from 3.7 to 4.3 (Sprules and Munawar, 1986). Note, however, that the methodology for obtaining size spectra for total particles differs from that used for living particles. For the total particles, a resistive-pulse particle counter is commonly used, while for living particles size measurements are mainly carried out by microscopy, gravimetry, or a combination of both (*e.g.*, Quiñones and Platt, 1992). Furthermore, in most cases only a small segment of the total particle size spectrum has been measured.

Here, the backscattering ratio was computed through equation (4.2), using equation (4.3) for $f(x)$ (with the corresponding change of variable) and integrating numerically over the size parameter range. The efficiency factors Q_b and Q_{b_b} were obtained from Mie theory with computer code according to Bohren and Huffman (1983). This code does not give Q_{b_b} directly but allows it to be computed by the integration of the given Mie intensity functions over the scattering angles $\pi/2 \leq \theta \leq \pi$. Computations were carried out on a NeXT workstation. Gradual underflow, provided in the IEEE arithmetic standard, allowed iterative calculations for the integrations to converge within accepted errors ($\leq$ 0.01%). Note that the limits of integration in equation (4.2) affect significantly $\tilde{b}_b'$, particularly the lower limit, since

$$\lim_{x\to 0} f(x) = \lim_{D\to 0} f(D) = \infty \,. \tag{4.4}$$

As shown in Figure 4.1, the backscattering ratio increases significantly when D_{min} is < 1 μm, clearly indicating that it is mainly controlled by sub-micrometer particles. Below a certain diameter ($\sim$ 0.05 μm), the backscattering ratio remains almost constant, indicating that particles with diameter lower than this value do not play any significant role in the backscattering process. From these results, the lower limit of integration was chosen to be 10^{-2} μm. For the upper limit we have

$$\lim_{x\to \infty} f(x) = \lim_{D\to \infty} f(D) = 0 \,, \tag{4.5}$$

and particles with $D \geq 100$ μm contribute $< 1\%$ to the backscattering and total scattering coefficients (Morel, 1973; Morel and Ahn, 1991; Stramski and Kiefer, 1991) and hence to the backscattering ratio. Here, D_{max} was fixed at 200 μm.

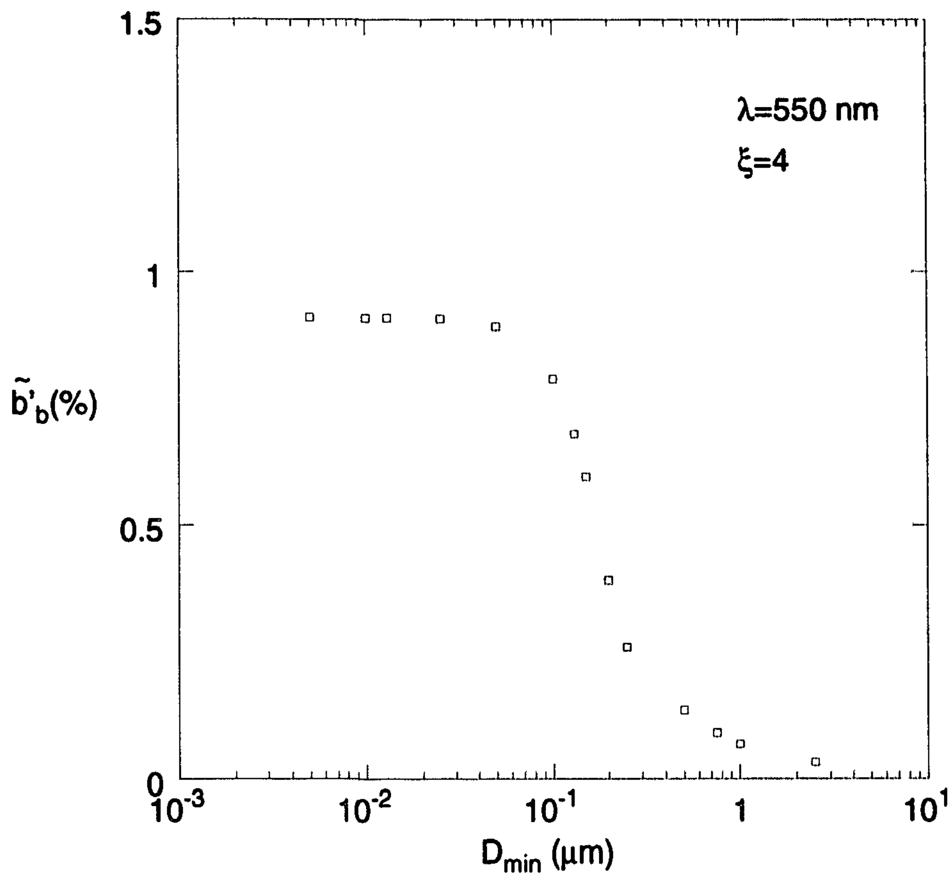

FIGURE 4.1. Effect of the lower limit of integration on the particle backscattering ratio ($\tilde{b}'_b$) for $m = 1.05 - 0.001i$ and $D_{max} = 200$ μm.

4.3 Influence of the Refractive Index and the Wavelength on the Backscattering Ratio

The backscattering ratio $\tilde{b}_b'$ was computed for different values of n and n', the real and imaginary part, respectively, of the refractive index m. Figure 4.2 shows that $\tilde{b}_b'$ increases with n, which can be attributed to the effect of the larger particles, since results for monodispersions show that the backscattering ratio for small particles ($x \leq\sim 2$ or $D \leq\sim 0.25$ μm at $\lambda = 550$ nm) is almost independent of the refractive index (both the real and imaginary parts), while for larger particles it is strongly dependent on n (Morel and Bricaud, 1981*b*; see also Fig. 1.2*d*).

Contrary to the case for monodispersions, or polydispersions with a normal or log-normal distribution, (Morel and Bricaud, 1981*b*) the backscattering ratio increases with n' for a given n (Fig. 4.3), particularly for $n' \geq\sim 10^{-2}$. Below this value the backscattering ratio is almost independent of n'. Even strongly-absorbing particles like phytoplankton will have values of $n' \leq 10^{-2}$ (Morel and Bricaud, 1986), which can therefore be considered an upper limit to n' for the total particle suspension. Thus, the variation of $\tilde{b}_b'$ due to absorption (*i.e.*, due to n') would be negligible. A typical 'bulk' value for the real part of the refractive index of the particles was chosen to be 1.05, but computations were carried out for other values of n as well, for comparison. The imaginary part was fixed at 10^{-3}.

Figure 4.4 shows that the backscattering ratio for particles that obey a Junge-type distribution does not vary with wavelength over the visible range. These results contrast with those for monodispersions, which show that $\tilde{b}_b'$ can be highly dependent on the wavelength, depending on the size of the particles and their refractive index (see, for example, Fig. 1.2*d* and Morel and Bricaud, 1981*b*; 1986).

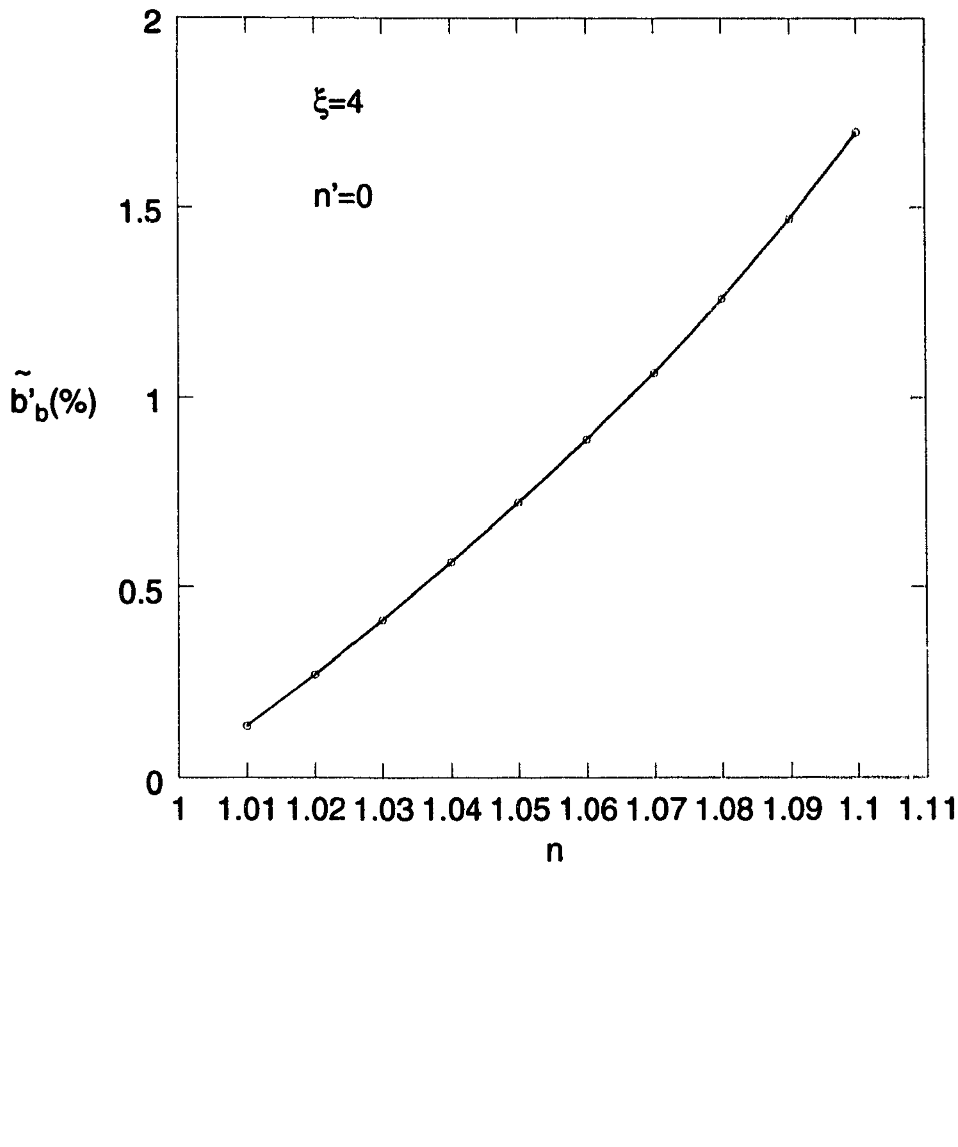

FIGURE 4.2. Effect of the real part of the refractive index (n) on the particle backscattering ratio ($\tilde{b}'_b$).

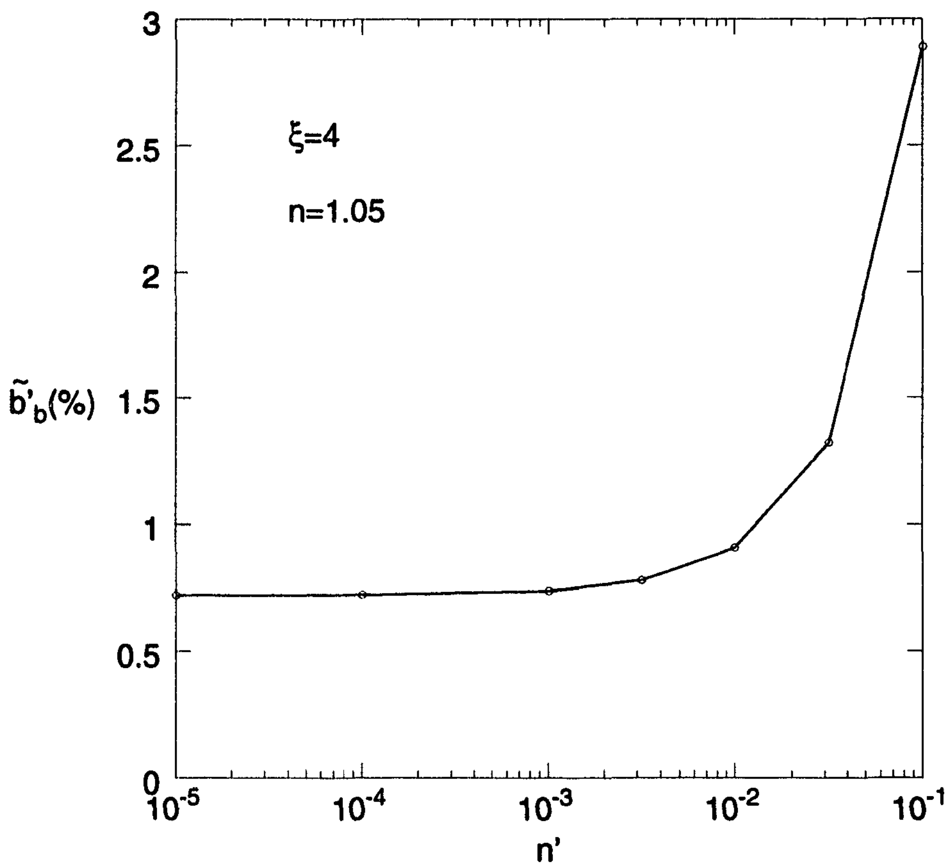

FIGURE 4.3. Effect of the imaginary part of the refractive index (n') on the particle backscattering ratio ($\tilde{b}'_b$).

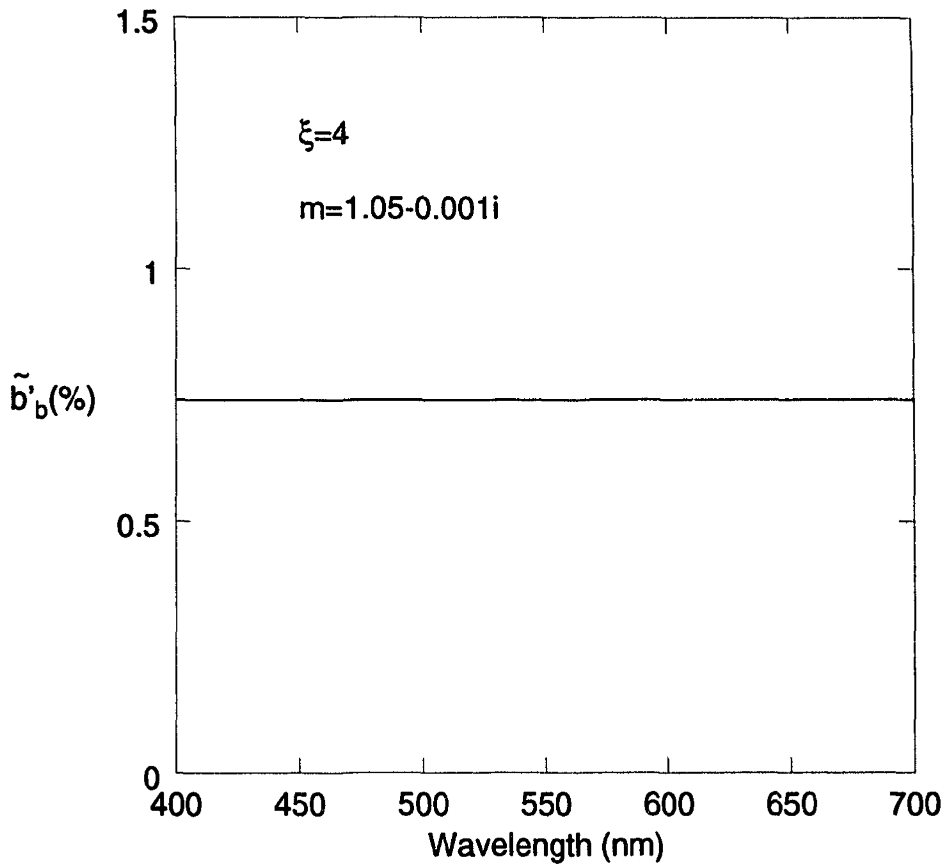

FIGURE 4.4. The backscattering ratio as a function of wavelength for particles with a Junge-type distribution; $D_{\min} = 10^{-2}$ μm and $D_{\max} = 200$ μm.

4.4 Influence of ξ

Once the limits of integration have been fixed, as discussed previously, changes in the size distribution $f(D)$ (equation 4.3) can only occur through changes in the coefficient ξ. Values of $\tilde{b}_b'$ were computed for the range of values reported for ξ in the literature. Results show (Fig. 4.5) that $\tilde{b}_b'$ is highly dependent on ξ and that this dependence increases with n; when $m = 1.05 - 0.001i$ the backscattering ratio varies according to $\sim \xi^{8.6}$, while for $m = 1.06 - 0.001i$ it varies according to $\sim \xi^{9.6}$. This strong dependence of $\tilde{b}_b'$ on ξ suggests that differences in the backscattering ratio in natural waters can arise from changes in the slope of the size spectrum of the total particle suspension. Waters with a higher ξ (a more negative slope) will have higher backscattering ratios, and *vice versa*. Moreover, these results indicate that ξ cannot be too large in natural waters, otherwise the backscattering ratio would be much higher than the 1–2% obtained from measurements of the volume scattering function or deduced from measurements of the spectral reflectance (Morel and Prieur, 1975; Gordon and Morel, 1983; Sathyendranath *et al.*, 1989).

4.5 Discussion

4.5.1 Influence of Small Particles.

In this chapter the backscattering ratio for polydispersions with a Junge-type distribution has been modelled using Mie theory. It was shown that if the size distribution of particles varies according to $D^{-\xi}$, where ξ is ~ 4, the backscattering ratio is largely controlled by sub-micrometer particles and that its magnitude does not vary with wavelength, nor is it significantly affected by absorption. Moreover, results indicate that the backscattering ratio varies strongly with the coefficient ξ. These results, however, are highly dependent on the assumption that the particle concentration continues to increase as the diameter becomes smaller than 1 μm.

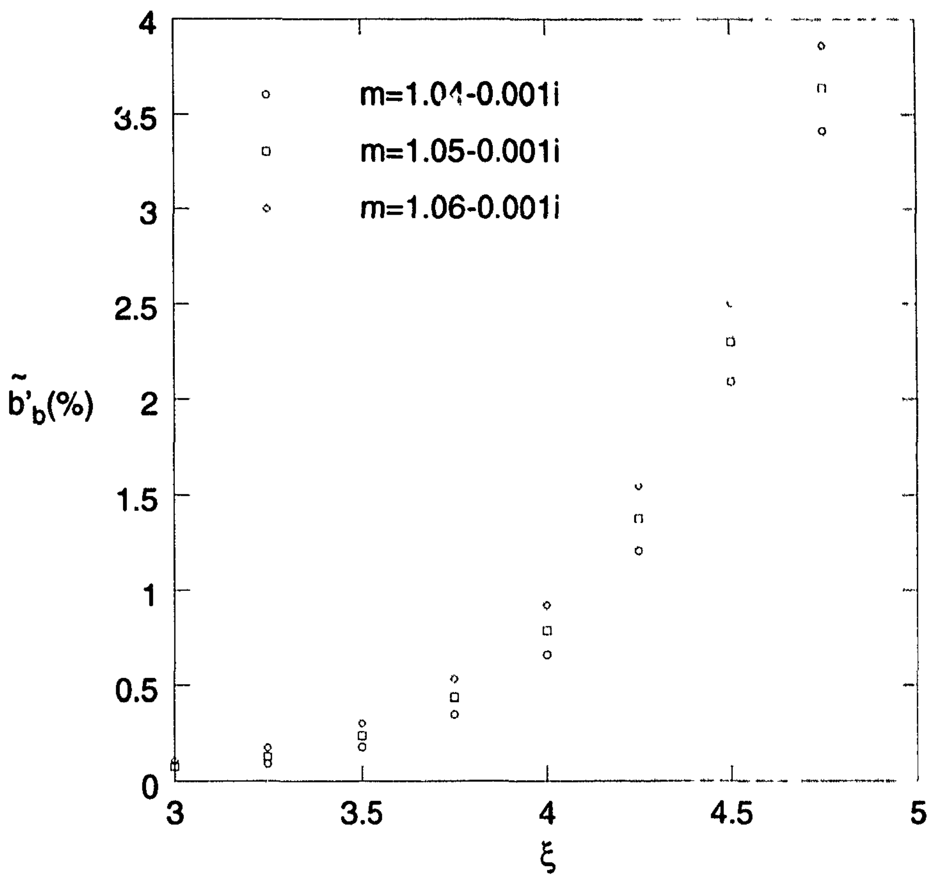

FIGURE 4.5. Effect of ξ on the particle backscattering ratio.

Direct evidence for the existence of a large concentration of sub-micrometer particles has only recently been obtained (Koike *et al.*, 1990; Longhurst *et al.*, 1992), but their existence has been predicted by optical models since the early seventies (Gordon and Brown, 1972; Brown and Gordon, 1973, 1974).

Gordon and Brown (1972) found that Kullenberg's (1968) data on the volume scattering function $\beta(\theta)$ at 632.8 nm could be reproduced using a Junge-type particle size distribution, with $\xi = 4$ and a single value for the refractive index $m = 1.05 - 0.01i$, typical of organic particles. However, to reproduce the observed backscattering ($\beta(\theta > 90^o)$) they had to assume the presence of a large number of sub-micrometer particles. They did not have simultaneous measurements of the size distribution, but they used other particle size data for the region (Bader, 1970), with a lower-end limit of 1 μm. Subsequently, Brown and Gordon (1973) used a two-component model (organic particles with $m = 1.01 - 0.01i$ and $0.1 \leq D \leq 2.5$ μm, and inorganic particles with $m = 1.15$ and $2.5 \leq D \leq 10$ μm, both with $\xi = 4$) to reproduce Kullenberg's data. Their results still showed that a large fraction of the suspended particle volume had to be of organic nature and of small size. Later, Brown and Gordon (1974) used simultaneous measurements of size distribution and volume scattering function to study the problem; the lower size limit of their Coulter Counter data was 0.65 μm. They could reproduce the volume scattering function at 488 nm using a three-component model, with inorganic particles in the middle-size class ($1.25 \leq D \leq 3.75$ μm) and organic particles in two classes of small and large sizes ($0.65 \leq D \leq 1.25$ μm and $3.75 \leq D \leq 17.0$ μm, respectively). However, the model could not reproduce the variation of $\beta(\theta)$ with wavelength. To achieve this, they had to include smaller particles of organic origin, or inorganic particles with a much smaller value for ξ. Regarding the small organic particles, they wrote: "...The prediction of the existence of vast quantities of small organic particles cannot be verified at this time, since little is known about sea water organics in these small sizes". Morel (1973), on the other hand, found that the average of several measured phase functions (or normalized volume scattering function) for marine particles could be reproduced with a Junge-type distribution with $\xi = 4$, $m = 1.05$, and $0.2 \leq x \leq 100$, *i.e.*, assuming implicitly the presence of sub-micrometer particles, which followed the same distribution as the larger particles.

Recently, Morel and Ahn (1991) and Stramski and Kiefer (1991) showed that if particles obey a Junge-type distribution with slope ~ -4 most of the total scattering would be due to particles with $1 \leq D \leq 10$ μm, while most of the backscattering would be due to particles < 1 μm. Although phytoplankton abundance, size ranges, and optical properties are such that they they can contribute significantly to the total scattering coefficient, they cannot account for the required backscattering. Furthermore, heterotrophic bacteria, which are in the sub-micrometer size range, and in concentrations of at least an order of magnitude higher than phytoplankton, can only account for a certain fraction of the backscattering coefficient (see also Chapter 3), but not for most of it. Both groups suggested that the possible component responsible for most of the backscattering in the ocean is very small, organic, detrital particles.

If indeed sub-micrometer particles are the main contributors to the backscattering in the ocean, the implications for our understanding of optical processes in the ocean are significant, since it has been commonly assumed that phytoplankton are the main contributors to the optical properties of sea water. Furthermore, optical properties are usually modelled in terms of phytoplankton pigment concentration (Sathyendranath and Platt, 1988; Gordon *et al.*, 1988; Morel, 1988). However, theoretical results, including those presented in this chapter, stress the importance of extremely small particles other than phytoplankton. Nevertheless, it remains to be established whether the presence of extremely small particles in great abundance is a common phenomenon in the ocean, and whether indeed particles follow a Junge-type distribution at the lower end of the size spectrum. Note that the lower end of detection of the resistive-pulse particle counters presently used to characterize these sub-micrometer particles is not better than 0.32 μm (Longhurst *et al.*, 1992), while the theoretical computations carried out here (and those discussed above) require that the abundance of the small particles continues to increase as the diameter diminishes to at least 0.1 μm (Fig. 4.3).

As it was mentioned in the introduction, the backscattering ratio is commonly used to estimate the backscattering coefficient from total scattering coefficient, equation (4.1), since a large body of experimental results exist relating its variation to that in the phytoplankton pigment concentration (Gordon and Morel, 1983). Here, the approach has been to study the dimensionless backscattering ratio, about which we know much less, to understand the sources of its variability and to examine whether the assumption of its dependence on pigment concentration (Gordon *et al.*; 1988; Morel *et al.*, 1988) has any theoretical, or empirical justification. The results indicate that a major source of variability in the backscattering ratio would be the shape of the total particle size distribution, parameterized here by the coefficient ξ in the Junge-type distribution.

4.5.2 Relationship Between ξ and Chlorophyll.

Sprules and Munawar (1986) analysed biomass size spectra from different lakes and included the results of Rodriguez and Mullin (1986) for the Central Gyre in the North Pacific for comparison. Their compilation showed that ξ decreases (the slope becomes more positive) with chlorophyll concentration. Recently, Quiñones (1992) carried out a detailed study of the biomass size distribution in the North Western Atlantic. His measurements covered a size range from bacteria to zooplankton ($\sim$ 0.5 to 1000 μm), and is probably the most extensive size range covered until today. Contrary to Sprules and Munawar (1986), the same methodology was used for obtaining the size spectra for the different locations. The size data in the study of Quiñones (1992) were well described by equation (4.3), as indicated by the coefficient of determination (all $r^2 \geq 0.9$). The computed slopes in phytoplankton-rich coastal waters (Georges Bank and Gulf of Maine) were significantly more positive (ξ lower) than in oligotrophic waters (Sargasso Sea and New England Seamounts), consistent with the results of Sprules and Munawar (1986). On the other hand, Kitchen, Zaneveld, and Pak (1982), studied the effect of the total particle size distribution and chlorophyll content on the beam attenuation spectra, and also found a significant negative correlation between the slope of the total particle size distribution and the chlorophyll concentration. Size measurements were carried out with a resistive-pulse particle counter covering equivalent spherical diameters between 1.6 and 32 μm.

The empirical studies on living and total particles mentioned above indicate that an inverse relationship exists between the coefficient ξ and the chlorophyll concentration. The strong direct relationship between ξ and $\tilde{b}_b'$ (Fig. 4.5) evident in my results clearly suggests an inverse relationship between the backscattering ratio and chlorophyll concentration. Therefore, even if most of the backscattering is due to non-phytoplanktonic particles of very small size, the backscattering ratio would vary inversely with chlorophyll concentration due to the inverse relationship that seems to exist between the slope of the size distribution and the chlorophyll concentration.

Optical models, like those use for the study of ocean colour by remote sensing (Gordon, 1988; Morel, 1988; Sathyendranath and Platt, 1988), presently work with the assumption that a relationship exists between the backscattering coefficient and the phytoplankton pigment concentration. On the other hand, theoretical studies suggest that most of the backscattering would be due to sub-micrometer detrital particles and not phytoplankton. Here I have offered an explanation to this aparent contradiction. An inverse relationship between the backscattering ratio and phytoplankton pigment concentration is possible due the observed inverse relationship between pigments and the shape of the total particle size distribution, which in turn is the principal control on the backscattering ratio.

General Discussion and Conclusions

The modelling of the behaviour of light in the ocean and the accurate interpretation of optical measurements obtained by remote sensing and by *in situ* optical sensors on profilers, moorings, and drifters, require some knowledge of the optical properties of the different substances present in sea water. Considerable attention, in this respect, has been paid to the study of the absorption and scattering characteristics of phytoplankton, which are considered (along with their derived products) to be the main contributors to the optical properties of sea water. The focus of this thesis, on the other hand, has been the much-less-studied, non-chlorophyllous particles, particularly the heterotrophic bacteria, and also the recently reported, sub-micrometer, detrital particles (Koike *et al.*, 1990; Longhurst *et al.*, 1992).

To estimate the relative contribution of heterotrophic bacteria to the scattering properties of sea water, Mie theory was applied to detailed measurements of bacterial size and abundance. Since no measurements of their refractive index were carried out during the cruise in which data on their size and abundance were collected, it was necessary to use values from the literature (Morel and Ahn, 1990; Stramski and Kiefer, 1990). These values had not been obtained by direct measurements, but deduced from optical measurements using a method (Stramski *et al.*, 1988) based on the approximations of van de Hulst (1957). It was necessary, therefore, to evaluate first the errors incurred in deriving them using these approximations instead of the exact Mie solutions (Chapter 1). Furthermore, the van de Hulst approximations had been used by Morel and Ahn (1990, 1991) to construct expressions for estimating bacterial scattering and absorption from phytoplankton pigment data, and to predict their potential contribution to the scattering and absorption coefficients in natural waters based on laboratory measurements.

In Chapter 1, it was shown that the approximations of van de Hulst are not always valid for the deduction of the refractive index of bacteria or for the estimation of their optical properties in the field, mainly because their size parameter range lies, in part, outside the range for which the approximations are valid. Furthermore, methods that use the van de Hulst approximation for Q_c (the efficiency factor for attenuation) to estimate the real part of the refractive index of particles from measurements of the attenuation coefficient (*e.g.*, Stramski *et al.*, 1988) cannot give reliable information over a significant portion of the size parameter range, therefore limiting their applicability to a restricted region of the particle size spectrum. It may be concluded from these results that models of the bacterial light scattering and absorption should, in principle, use Mie theory to compute the corresponding optical coefficients, rather than the van de Hulst approximations.

Mie computations, however, are time consuming, and can become impractical when the results have to be incorporated into other bio-optical models, which in turn are very demanding in computational time, for example, in the calculation of primary production from remotely sensed data (Platt and Sathyendranath, 1988). With this in mind, two simple approximations were derived for the bacterial scattering coefficient (Chapter 2), one for the case in which the bacterial size distribution is skewed, and can be represented by a gamma distribution, and the other one for the case in which it is symmetrical with respect to the mean, and can be represented by a normal distribution. Results from measurements of bacterial size distributions using epifluorescence microscopy showed that both distributions represent field data well. The derived approximations are improvements over previous ones (Morel and Ahn, 1990), in the sense that they are based on Mie theory rather than on the van de Hulst approximations, and that they are not restricted to monodispersions.

The use of Mie theory in this thesis to describe bacterial scattering was based on the assumption that heterotrophic bacteria are spherical particles. Results of their size measurements (Chapter 3) showed that this is not strictly the case for all bacteria (Figure 3.2). Theoretical analyses of the light scattering properties of spheroidal particles show that their efficiency factors for scattering and attenuation deviate gradually from those of spheres of the same volume with increase in the ratio of major axis to minor axis (Asano and Yamamoto, 1975; Asano, 1979). For randomly oriented spheroids, which can be considered to be the case of bacteria in the ocean, the efficiency factors for scattering and attenuation tend to be higher than those for spheres of the same volume, but the efficiency factor for absorption is almost equal (Asano and Sato, 1980). Results from these analyses would indicate that in this study the contribution of heterotrophic bacteria to the scattering coefficient would have been underestimated.

However, for randomly oriented spheroidal particles with sizes lower than the first maximum in the scattering (or attenuation) curve for spheres (Fig. 1.2*a*), Asano and Sato (1980) showed that the efficiency factor for scattering (or attenuation) is primarily dependent on the size and weakly dependent on the shape, and therefore it is very close to that for spheres. Thus, considering that the size parameter range representative of bacteria lies clearly below the first maximum in the scattering (or attenuation) curve (Chapter 1), it is concluded that the errors introduced in the computation of their scattering coefficient by assuming sphericity would be only nominal.

The scattering properties of heterotrophic bacteria were computed in three marine environments that varied in almost 2 orders of magnitude in the phytoplankton pigment concentration (Chapter 3). It was found that bacteria can make significant contributions to both the total scattering coefficient and the backscattering coefficient, but that their contribution to the backscattering coefficient was relatively smaller. Furthermore, it was found that there was no relationship between the degree to which bacteria contributed to the scattering properties and the the amount of phytoplankton pigments present in the water.

These results, hence, did not support previous theoretical predictions which indicated that bacterial scattering relative to total scattering would be more important in waters that have a higher concentration of bacteria (Kopelevich *et al.*, 1987), that their relative contribution would be independent of the amount of pigments (Morel and Ahn, 1990), or that they would be more important contributors in the oligotrophic ocean (Stramski and Kiefer, 1990). Part of the problem with these earlier predictions was that a relationship was assumed between the concentration of heterotrophic bacteria and the phytoplankton pigment concentration. As it was shown here, this assumption is not valid, at least for the data set examined. Note, however, that the data presented here came from different marine ecosystems and the number of points in the regression in Figure 3.5 ($N = 364$) was much higher than in previous studies which had postulated a relationship between bacterial abundance and pigments (*e.g.*, Bird and Kalff, 1984; Cole *et al.*, 1988). Furthermore, other recent studies do not support the idea that bacterial numbers covary with phytoplankton pigment concentration (*e.g.*, Karl *et al.*, 1991). Consequently, the bacterial contribution to the scattering coefficient will have to be considered independently from that of phytoplankton.

These results have significant implications for the interpretation of optical data. For example, Siegel *et al.* (1989) proposed that phytoplankton growth rates can be estimated from changes in the attenuation coefficient measured with transmissometers. Accurate estimates of their growth rates, however, require knowledge of the relative contribution of phytoplankton, microheterotrophs and detritus to the attenuation process (Cullen *et al.*, 1992). Since variations in the attenuation coefficient can be mainly controlled by scattering (as opposed to absorption) at the wavelengths used with the transmissometers (*e.g.*, 660 nm, Siegel *et al.*, 1989; Cullen *et al.*, 1992), the contribution of bacteria cannot be neglected, or considered to be proportional to that of phytoplankton, and will have to be estimated independently.

For the modelling and interpretation of remotely-sensed data of ocean colour, on the other hand, it is necessary to consider the backscattering coefficient ($b_b(\lambda)$), since it is this optical property (in combination with the absorption coefficient $a(\lambda)$) which is related to the irradiance reflectance $R(\lambda)$, the ratio of upward to downward irradiance (see review by Gordon and Morel, 1983). For the case where $b_b/a << 1$, $R(\lambda)$ can be approximated by (Morel and Prieur, 1977)

$$R(\lambda) = 0.33 \left(\frac{b_b(\lambda)}{a(\lambda)} \right) .$$

Results in Chapter 3 showed that heterotrophic bacteria could contribute up to $\sim 20\%$ to the total backscattering coefficient b_b, but more typically their contribution would be $\leq 10\%$. Since b_b in the above equation is directly proportional to R, neglecting the independent contribution of bacteria to the backscattering coefficient would introduce relative errors in R of the same magnitude. On the other hand, theoretical and laboratory results (Morel and Ahn, 1991) show that the backscattering coefficient due to heterotrophic bacteria is independent of wavelength (λ). This implies that bacteria would not interfere with the phytoplankton pigment algorithms based on ratios of reflectance at different wavelengths, but they would affect those that rely on differences in R from one wavelength to another.

However, in current models of irradiance reflectance (Gordon *et al.*, 1988; Morel, 1988; Sathyendranath and Platt, 1988) the backscattering coefficient is obtained through the total scattering coefficient (see Chapters 3 and 4), more specifically, through an empirical relationship (equation (3.2)) between the total scattering coefficient and phytoplankton pigment concentration (Gordon and Morel, 1983). Although this empirical relationship (equation (3.2)) was shown to be statistically significant, the variance in the data was high; for a given concentration of pigments, values of the scattering coefficient in Case 1 waters varied 2–4 fold, and more than an order of magnitude in Case 2 waters. Variations in the chlorophyll-specific scattering coefficient of phytoplankton is generally considered to be responsible for this variance (Gordon *et al.*, 1988). The results presented here suggest an additional factor: variable bacterial contribution to the total scattering coefficient, which can be as low as 3% or as high as 60% (Chapter 3). Note again that this bacterial contribution does not covary with chlorophyll concentration, and would constitute noise in any model that ignores the role of bacteria.

A method for estimating bacterial contribution by remote sensing remains to be established. One possibility is that bacterial numbers may covary with the amount of yellow substances (dissolved organic material) present in the water, since these substances are used by bacteria as substrate for their metabolic activities. Supposedly, with the next generation of ocean colour sensors it will be possible to estimate the concentration of yellow substances (Sathyendranath *et al.*, 1989; Calder *et al.*, 1991).

The other optical property involved in the computation of the backscattering coefficient is the backscattering ratio (see equation (4.1)). Results in Chapter 4 showed that this ratio is largely controlled by the presence of sub-micrometer particles and that its magnitude is strongly dependent on the shape of the size distribution, parameterized here by the coefficient ξ in the Junge-type distribution. This latter coefficient has been shown empirically to be inversely related to the amount of phytoplankton pigments present in the water (Sprules and Munawar, 1986; Quiñones, 1992). Therefore, although sub-micrometer, non-phytoplanktonic particles would be largely responsible for the amount of backscattering in the ocean, it was concluded that the backscattering coefficient, and particularly the backscattering ratio, can be modelled in terms of the phytoplankton pigment concentration.

Whether sub-micrometer detrital particles are indeed the main backscatterers in the ocean remains to be confirmed. If that is the case, then efforts should be made to characterize their optical properties and their sources of variability in the ocean, since they would be the ones responsible for most of the signal reaching the sensors in space. A significant, but much lower, contribution would come from heterotrophic bacteria. They seem, however, to be important contributors to the total scattering coefficient. To account for their presence, it is necessary to estimate their concentration, which can presently be obtained only by direct counting. A challenge then is to estimate their concentration through remote sensing.

Future work should also consider the effect of non-chlorophyllous particles on the volume scattering function. Variations, for example, of R with the solar zenith angle have been shown to be strongly dependent on the shape of volume scattering function (Kirk, 1984; Morel and Gentili, 1991). The degree to which bacteria and sub-micrometer detrital particles affect the angular distribution of the submarine light field and light penetration in the ocean remains also to be established.

APPENDIX I

Computation of the Mie Scattering Coefficients

To compute the optical efficiency factors (equations (1.9 a-c)) and the angular intensity parameters (equations (1.10 a, b)) from Mie theory it is necessary to calculate the complex scattering coefficients $a_k(m, x)$ and $b_k(m, x)$, given by

$$a_k(m, x) = \frac{\psi_k(x)\psi_k'(y) - m\psi_k(y)\psi_k'(x)}{\zeta_k(x)\psi_k'(y) - m\psi_k(y)\zeta_k'(x)} ,$$

and

$$b_k(m, x) = \frac{m\psi_k(x)\psi_k'(y) - \psi_k(y)\psi_k'(x)}{m\zeta_k(x)\psi_k'(y) - \psi_k(y)\zeta_k'(x)} ,$$

where m is the (complex) refractive index, x is the (real) size parameter, $y = mx$, ψ_k and ζ_k are the Riccati-Bessel functions, and the primes denote differentiation with respect to the argument. The Riccati-Bessel functions are defined by

$$\psi_k(z) = zj_k(z) = \left(\frac{\pi z}{2}\right)^{1/2} J_{k+1/2}(z) ,$$

$$\zeta_k(z) = zh_k^{(2)}(z) = \psi_k(z) - i\chi_k(z) ,$$

$$\chi_k(z) = -zy_k(z) = (-1)^k \left(\frac{\pi z}{2}\right)^{1/2} J_{-k-1/2}(z) ,$$

where $j_k(z)$, $y_k(z)$, are the Spherical Bessel functions of the first and second kind, respectively (Abramowitz and Stegun, 1964), $i = \sqrt{-1}$, $h_k^{(2)}(z) = j_k(z) - iy_k(z)$, and $J_{k+1/2}(z)$ and $J_{-k-1/2}(z)$ are Bessel functions of the first kind of half-odd-integral order. The Spherical Bessel functions (summarily denoted by $z_k(z)$) satisfy the recurrence relations

$$z_{k-1}(z) + z_{k+1}(z) = \left(\frac{2k+1}{z}\right) z_k(z) \ ,$$

$$z'_k(z) = -\frac{k}{z} z_k(z) + z_{n-1}(z) \ ,$$

which can be used to to calculate Ricatti-Bessel functions of arbitrary order from the functions of the two preceeding orders.

However, the total number of terms, $k_{\rm max}$, required for convergence in the Mie series is of order x, and for large x the roundoff errors can accumulate in such a way as to yield incorrect results. Various computational methods for efficient Mie algorithms have been proposed. In this thesis, I used the one given in Bohren and Huffman (1983), which has been shown to agree with other codes to ~ 5 significant figures for x as large as $x = 500$, in the computation, for example, of the efficiency factors (Wang and van de Hulst, 1991).

In this code,

$$k_{\rm max} = x + 4x^{1/3} + 2 \ ,$$

and the scattering coefficients are obtained from

$$a_k(m,x) = \frac{[D_k(mx)/m + k/x]\psi_k(x) - \psi_{k-1}(x)}{[D_k(mx)/m + k/x]\zeta_k(x) - \zeta_{k-1}(x)} \ ,$$

and

$$b_k(m,x) = \frac{[mD_k(mx) + k/x]\psi_k(x) - \psi_{k-1}(x)}{[mD_k(mx) + k/x]\zeta_k(x) - \zeta_{k-1}(x)} \ ,$$

where $D_k(z) = d/dz \ln \psi_k(z)$ is the logarithmic derivative that satisfies the recurrence relation

$$D_{k-1} = \frac{k}{z} - \frac{1}{D_k + k/z} \, .$$

The calculations of $D_k(mx)$ are done by downward recurrence, while those of $\psi_k(x)$ and $\zeta_k(x)$ by upward recurrence, in both cases using double precision.

REFERENCES

Abramowitz, M., and I. A. Stegun, Eds. (1964). *Handbook of Mathematical Functions*, National Bureau of Standards, Washington, D.C.

Ackleson, S. G., and R. W. Spinrad (1988). Size and refractive index of individual marine particulates: A flow cytometric approach, *Appl. Opt.*, 27: 1270–1277.

Asano, S. (1979). Light scattering properties of spheroidal particles, *Appl. Opt.*, 18: 712–723.

Asano, S., and M. Sato (1980). Light scattering by randomly oriented spheroidal particles, *Appl. Opt.*, 19: 962–974.

Asano, S., and G. Yamamoto (1975). Light scattering by spheroidal particles, *Appl. Opt.*, 14: 29–49.

Bader, H. (1970). The hyperbolic distribution of particle sizes. *J. Geophys. Res.*, 75: 2822–2830.

Bateman, J. B., J. Wagman, and E. L. Carstensen (1966). Refraction and absorption of light in bacterial suspensions, *Kolloid Z. Z. Polym.*, 208: 44–58.

Bird, D. F., and J. Kalff (1984). Empirical relationships between bacterial abundance and chlorophyll concentration in fresh and marine waters, *Can. J. Fish. Aquat. Sci.*, 41: 1015–1023.

Bohren, C. F., and D. R. Huffman (1983). *Absorption and Scattering of Light by Small Particles*, John Wiley, New York.

Bricaud, A., and A. Morel (1986). Light attenuation and scattering by phytoplanktonic cells: a theoretical modeling, *Appl. Opt.*, 25: 571–580.

Bricaud, A., A. Morel, and L. Prieur (1983). Optical efficiency factors of some phytoplankters, *Limnol. Oceanogr.*, 28: 816–832.

Brown, O. B., and H. R. Gordon (1973). Two component Mie scattering models of Sargasso Sea particles, *Appl. Opt.*, 12: 2461–2465.

Brown, O. B., and H. R. Gordon (1974) Size-refractive index distribution of clear coastal water particulates from light scattering, *Appl. Opt.*, 13: 2874–2881.

Bryant, F. D., B. A. Seiber, and P. Latimer (1969). Absolute optical cross sections of cells and chloroplasts, *Arch. Biochem. Biophys.*, 135: 97–108.

Calder, K. L., S. K. Hawes, K. A. Baker, R. C. Smith, R. G. Steward, and B. G. Mitchell (1991). Reflectance model for quantifying chlorophyll *a* in the presence of productivity degradation products, *J. Geophys. Res.*, 96: 20599–20611.

Campana, S. E. (1987). Image analysis for microscope-based observations: An inexpensive configuration, *Can. Tech. Rep. Fish. Aquat. Sci.*, 1569: iv+20 pp.

Cho, B. C., and F. Azam (1990). Biogeochemical significance of bacterial biomass in the ocean's euphotic zone, *Mar. Ecol. Prog. Ser.*, 63: 253–259.

Chýlek, P. (1973). Mie scattering in the backward hemisphere, *J. Opt. Soc. Am.*, 63: 1467–1471.

Chýlek, P., P. Damiano, D. Ngo, and R. G. Pinnick (1992). Polynomial approximation of the optical properties of water clouds in the 8-12-μm spectral region, *Appl. Meteor.*, 31: 1210–1218.

Chýlek, P., P. Damiano, and E. P. Shettle (1992). Infrared emittance of water clouds, *J. Atmos. Sci.*, 49: 1459–1472.

Cole, J. J., S. Findlay, and M. L. Pace (1988). Bacterial production in fresh and salt water ecosystem: A cross-system overview, *Mar. Ecol. Prog. Ser.*, 43: 1–10.

Cullen, J. J., M. R. Lewis, C. O. Davis, and R. Barber (1992). Photosynthetic characteristics and estimated growth rates indicate grazing is the proximate control of primary production in the Equatorial Pacific, *J. Geophys. Res.*, 97: 639–654.

Damiano, P. (1992). Parameterization of the Radiative Properties of Water Clouds in the Solar and Terrestial Wavelength Regions, *M.Sc. Thesis*, Dalhousie University, Halifax.

Deirmendjian, D. (1969). *Electromagnetic Scattering on Spherical Polydispersions*, Elsevier, New York.

Ducklow, H. (1986). Bacterial biomass in warm-core Gulf Stream ring 2-B: Mesoscale distribution, temporal changes and production, *Deep-Sea Res.*, 33: 1789–1812.

Duysens, L. N. M. (1956). The flattening of the absorption spectrum of suspensions, as compared to that of solutions, *Biochim. Biophys. Acta*, 19: 1–12.

Frankel, S. L., B. J. Binder, S. W. Chisholm, and H. M. Shapiro (1990). A high-sensitivity flow cytometer for studying picoplankton, *Limnol. Oceanogr.*, 35: 1164–1169.

Fuhrman, J. A. (1981). Influence of method on the apparent size distribution of bacterioplankton cells: Epiflurescence microscopy compared to scanning electron microscopy, *Mar. Ecol. Prog. Ser.*, 5: 103–106.

Fuhrman, J. A., T. D. Sleeter, D. A. Carlson, and L. M. Proctor (1989). Dominance of bacterial biomass in the Sargasso Sea and its ecological implications. *Mar. Ecol. Prog. Ser.*, 57: 207–217.

Gordon, H. R., and O. B. Brown (1972). A theoretical model of light scattering by Sargasso Sea particulates, *Limnol. Oceanogr.*, 17: 826–832.

Gordon, H. R., and A. Y. Morel (1983). *Remote Assessment of Ocean Color for Interpretation of Satellite Visible Imagery: A Review*, 114 pp., Springer-Verlag, New York.

Gordon, H. R., O. B. Brown, and M. M. Jacobs (1975). Computed relationships between the inherent and apparent optical properties of a flat homogeneous ocean, *Appl. Opt.*, 14: 417–427.

Gordon, H. R., O. B. Brown, R. H. Evans, J. W. Brown, R. C. Smith, K. S. Baker, and D. K. Clark (1988). A semianalytic radiance model of ocean color, *J. Geophys. Res.*, 93: 10909–10924.

Gradshteyn, I. S., and I. M. Rhyzhik (1980). *Table of Integrals, Series and Products. Corrected and Enlarged Edition*, Academic Press, San Diego.

Güde, H. (1989). The role of grazing on bacteria in plankton succession, in *Plankton Ecology: Succession in Plankton Communities*, edited by U. Sommer, pp. 337–364, Springer-Verlag, New York.

Irwin, B., J. Anning, C. Caverhill, M. Hodgson, A. Macdonald, and T. Platt (1990*a*). Primary production on Georges Bank—August 1988, *Can. Data Rep. Fish. Aquat. Sci.*, 785, iv+197 pp.

Irwin, B., J. Anning, C. Caverhill, M. Hodgson, A. Macdonald, and T. Platt (1990*b*). Primary production in the northern Sargasso Sea in September 1988, *Can. Data Rep. Fish. Aquat. Sci.*, 798, iv+93 pp.

Jerlov, N. G. (1976). *Marine Optics*, Elsevier, New York.

Jonasz, M. (1983). Particle-size distributions in the Baltic, *Tellus*, 35B: 346–358.

Karl, D. M., O. Holm-Hansen, G. T. Taylor, G. Tien, and D. F. Bird (1991). Microbial biomass and productivity in the western Bransfield Strait, Antarctica during the 1986–87 austral summer, *Deep-Sea Res.*, 38: 1029–1055.

Kishino, M. (1980). Studies of the optical properties of sea water. Application of Mie theory to suspended particles in sea water, *Sci. Pap., Inst. Phys. Chem. Res.*, 74: 31–45.

Kirk, J. T. O. (1983). *Light and Photosynthesis in Aquatic Ecosystems*, Cambridge University Press, New York.

Kirk, J. T. O. (1984). Dependence of relationship between inherent and apparent optical properties of water on solar altitude, *Limnol. Oceanogr.*, 29: 350–356.

Kirk, J. T. O. (1988). Solar heating of water bodies as influenced by their inherent optical properties, *J. Geophys. Res.*, 93: 10897–10908.

Kishino, M. (1980). Studies of the optical Properties of sea water. Application of Mie theory to suspended particles in sea water, *Sci. Pap., Inst. Phys. Chem. Res.*, 74: 31–45.

Kitchen, J. C., and J. R. V. Zaneveld (1990). On the noncorrelation of the vertical structure of light scattering and chlorophyll *a* in case I waters, *J. Geophys. Res.*, 95: 20237–20246.

Koch, A. L. (1968). Theory of the angular dependance of light scattered by bacteria and similar-sized objects, *J. Theor. Biol.*, 18: 133–156.

Kogure, K., and I. Koike (1987). Particle counter determination of bacterial biomass in seawater, *Appl. Environ. Microbiol.*, 53: 274–277.

Koike, I., S. Hara, T. Terauchi, and K. Kogure (1990). Role of sub-micrometer particles in the ocean, *Nature*, 345: 242–244.

Kopelevich, O. V., V. V. Rodionov, and T. P. Stupakova (1987). Effect of bacteria on optical characteristics of ocean water, *Oceanology, Engl. Trans.*, 27: 696–700.

Kullenberg, G. (1968). Scattering of light by Sargasso Sea water, *Deep-Sea Res.*, 15: 423–432.

Lewis, M. R., J. J. Cullen, and T. Platt (1983). Phytoplankton and termal structure in the upper ocean: Consequences of nonuniformity in chlorophyll profile, *J. Geophys. Res.* 88: 2565–2570.

Li, W. K. W., P. M. Dickie, B. D. Irwin, and A. M. Wood (1992). Biomass of bacteria, cyanobacteria, prochlorophytes and photosynthetic eukaryotes in the Sargasso Sea, *Deep Sea Res.*, 39: 501–519.

Linley, E. A. S., R. C. Newell, and M. I. Lucas (1983). Quantitative relationships between phytoplankton, bacteria and heterotrophic microflagellates in shelf waters, *Mar. Ecol. Prog. Ser.*, 12: 77–89.

Longhurst, A. R., I. Koike, W. K. W. Li, J. Rodriguez, P. Dickie, P. Kepkay, F. Partensky, B. Bautista, J. Ruiz, M. Wells, and D. F. Bird (1992). Sub-micron particles in northwest Atlantic shelf water, *Deep-Sea Res.*, 39: 1–7.

McManus, G. B., and W. T. Peterson (1988). Bacterioplankton production in the nearshore zone during upwelling off central Chile, *Mar. Ecol. Prog. Ser.*, 43: 11-17.

Mie, G. (1908). Beiträge zur Optik trüber Medien, Speziell kolloidalen Metallösungen, *Ann. Phys.*, 25: 377–445.

Moore, D. M., F. D. Bryant, and P. Latimer (1968). Total scattering and absorption by spheres where $m \cong 1$. *J. Opt. Soc. Am.*, 58: 281–283.

Morel, A. (1973). Diffusion de la lumière par les eaux de mer. Résultats expérimentaux et approche théorique, in *Optics of the Sea, AGARD Lect. Ser.*, vol. 61, pp. 3.1.01–3.1.76, Advisory Group for Aeronautical Research and Development, NATO, Brussels.

Morel, A. (1974). Optical properties of pure water and pure sea water, in *Optical Aspects of Oceanography*, edited by N. G. Jerlov and E. Steemann Nielsen, pp. 1–24, Academic Press, San Diego

Morel, A. (1988). Optical modelling in the upper ocean in relation to its biogenous matter content (Case I waters), *J. Geophys. Res.*, 93: 10,749–10,768.

Morel, A., and Y.-H. Ahn (1990). Optical efficiency factors of free-living marine bacteria: Influence of bacterioplankton upon the optical properties and particulate organic carbon in oceanic waters, *J. Mar. Res.*, 48: 145–175.

Morel, A., and Y.-H. Ahn (1991). Optics of heterotrophic nanoflagellates and ciliates: A tentative assessment of their scattering role in oceanic waters compared to those of bacteria and algal cells, *J. Mar. Res.*, 49: 177–202.

Morel A., and A. Bricaud (1981*a*). Theoretical results concerning light absorption in a discrete medium, and application to specific absorption of phytoplankton, *Deep-Sea Res.*, 28: 1375–1393.

Morel, A., and A. Bricaud (1981*b*). Theoretical results concerning the optics of phytoplankton, with special reference to remote sensing applications, in *Oceanography From Space*, edited by J. F. R. Gower, pp. 313–327, Plenum, New York.

Morel, A., and A. Bricaud (1986). Inherent optical properties of algal cells including picoplankton: Theoretical and experimental results, *Can. Bull. Fish. Aquat. Sci.*, 214: 521–559.

Morel, A., and B. Gentili (1991). Diffuse reflectance of oceanic waters: its dependence on Sun angle as influenced by the molecular scattering contribution, *Appl. Opt.*, 30: 4427–4438.

Morel, A., and L. Prieur (1977). Analysis of variations in ocean color, *Limnol. Oceanogr.*, 22: 709–722.

Petukhov, V.G. (1965). The feasibility of using the Mie theory for the scattering of light from suspensions of spherical bacteria (in Russian), *Biofizika*, 10: 993–999.

Petzold, T. J. (1972). Volume scattering functions for selected ocean waters, *SIO Ref. 72-28*, 79 pp., Scripps Inst. of Oceanogr., La Jolla, Calif.

Platt, T, and K. Denman (1977). Organization in the pelagic ecosystem. *Helgol. Wiss. Meeresunters.*, 30: 575-581.

Platt, T, and K. Denman (1978). The structure of pelagic ecosystems. *Rapp. P-V. Reun. Cons. Int. Explor. Mer*, 173: 60–65.

Platt, T., and S. Sathyendranath (1988). Oceanic primary production: Estimation by remote sensing at local and regional scales, *Science*, 241: 1613–1620.

Platt, T., M. Lewis, and R. Geider (1984). Thermodynamics of the pelagic ecosystem: Elementary closure conditions for biological production in the open ocean, in *Flows of Energy and Material in Marine Ecosystems*, edited by M. J. R. Fasham, pp. 49–84, Plenum Press, London.

Porter, K. G., and Y. S. Feig (1980). The use of DAPI for identifying and counting aquatic microflora, *Limnol. Oceanogr.*, 25: 943-948.

Preisendorfer, R. W. (1961). Application of radiative transfer theory to light measurements in the sea, *Monogr. 10*, pp. 11–30, Int. Union. of Geod. and Geophys., Paris.

Quiñones, R. A. (1992). Size-distribution of plankton biomass and metabolic activity in the pelagic system, *Ph.D. Thesis*, Dalhousie University, Halifax.

Quiñones, R. A., and T. Platt (1992). Patterns of biomass size-spectra from oligotrophic waters of the northwest Atlantic, *Mar. Ecol. Prog. Ser.*, in press.

Robertson, B. R., and D. K. Button (1989). Characterizing aquatic bacteria according to population, cell size, and apparent DNA content by flow cytometry, *Cytometry*, 10: 70–76.

Rodriguez, J., and M. Mullin (1986). Relatio between biomass and body weight of plankton in a steady state oceanic ecosistem, *Limnol. Oceanogr.*, 31: 361–370.

Sathyendranath, S., and T. Platt (1988). The spectral irradiance field at the surface of the ocean: A model for application in oceanography and remote sensing, *J. Geophys. Res.*, 93: 9270–9280.

Sathyendranath, S., L. Prieur, and A. Morel (1989). A three-component model of ocean colour and its application to remote sensing of phytoplankton pigments in coastal waters, *Int. J. Remote Sensing*, 10: 1373–1394

Sheldon, R. W., A. Prakash, and W. H. Jr. Sutcliffe (1972). The size distribution of particles in the ocean, *Limnol. Oceanogr.*, 17: 327–340.

Shimizu, K., and A. Ishimaru (1978). Scattering pattern analysis of bacteria, *Opt. Eng.*, 17: 129–134.

Siegel, D. A., T. D. Dickey, L. Washburn, M. K. Hamilton, and G. G. Mitchel (1989). Optical determination of particulate abundance and production variations in the oligotrophic ocean, *Deep-Sea Res.*, 36: 211-222.

Spinrad, R. W., H. Glover, B. B. Ward, L. A. Codispoti, and G. Kullenberg (1989*a*). Suspended particle and bacteria maxima in Peruvian coastal waters during a cold water anomaly, *Deep-Sea Res.*, 36: 715–733.

Spinrad, R. W., C. M. Yentsch, J. Brown, Q. Dortch, E. Haugen, N. Revelante, and L. Shapiro (1989*b*). The response of beam attenuation to heterotrophic growth in a natural population of plankton, *Limnol. Oceanogr.*, 34: 1601–1605.

Sprules, W. G., and M. Munawar (1986). Plankton size spectra in relation to ecosystem productivity, size, and perturbation, *Can. J. Fish. Aquat. Sci.*, 43: 1789–1794.

Sheldon, R. W., A. Prakash, and W. H. Jr. Sutcliffe (1972). The size distribution of particles in the ocean, *Limnol. Oceanogr.*, 17: 327–340.

Stramski, D., and D. A. Kiefer (1990). Optical properties of marine bacteria, *Proc. Soc. Photo. Opt. Instrum. Eng., Ocean Opt. X*, 1302: 250–268.

Stramski, D., and D. A. Kiefer (1991). Light scattering by microorganisms in the open ocean, *Prog. Oceanog.*, 28: 343–383.

Stramski, D., and A. Morel (1990). Optical properties of photosynthetic picoplankton in different physiological states as affected by growth irradiance, *Deep-Sea Res.*, 37: 245–266.

Stramski, D., A. Morel, and A. Bricaud (1988). Modeling the light attenuation by spherical phytoplanktonic cells: A retrieval of the bulk refractive index, *Appl. Opt.*, 27: 3954–3956.

Ulloa, O., S. Sathyendranath, T. Platt, and R. A. Quiñones (1992). Light scattering by marine heterotrophic bacteria, *J. Geophys. Res.*, 97: 9619–9629.

van de Hulst, H. C. (1957). *Light Scattering by Small Particles*, John Wiley, New York.

Wang, R. T., and H. C. van de Hulst (1991). Rainbows: Mie computations and the Airy approximation, *Appl. Opt.*, 30: 106–117.

Yentsch, C. S. (1962). Measurements of visible light absorption by particulate matter in the ocean, *Limnol. Oceanogr.*, 7: 207–217.

Zaneveld, J. R. V., J. C. Kitchen, and H. Pak (1981). The influence of optical water type on the heating rate of a constant depth mixed layer, *J. Geophys. Res.*, 86: 6424–6428.

Zaneveld, J. R. V., D. M. Roach, and H. Pak (1974). The determination of the index of refraction distribution of oceanic particles, *J. Geophys. Res.*, 79: 4091–4095.